2012

Postglacial climate, disturbance and permafrost peatland dynamics on the Seward Peninsula, Western Alaska

Stephanie Julia Hunt
Lehigh University

POSTGLACIAL CLIMATE, DISTURBANCE AND PERMAFROST PEATLAND DYNAMICS ON THE SEWARD PENINSULA, WESTERN ALASKA

By

Stephanie Hunt

A Thesis

Presented to the Graduate and Research Committee

of Lehigh University

in Candidacy for the Degree of

Masters of Science

in

Earth and Environmental Sciences

Lehigh University

April 25, 2012

Thesis is accepted and approved in partial fulfillment of the requirements for the Master of Science in Earth and Environmental Sciences

Title: "Postglacial Climate, Disturbance and Permafrost Peatland Dynamics on the Seward Peninsula, Western Alaska"

Stephanie Hunt

Date Approved

Zicheng Yu

Advisor

Robert Booth

Committee Member

Benjamin Felzer

Committee Member

Frank Pazzaglia

Department Chair Person

ACKNOWLEDGMENTS

I would like to thank my committee, Zicheng Yu, Bob Booth, and Ben Felzer, for their support, discussion, and comments throughout my course of study. I also thank Miriam Jones for discussion and comments. I thank Chris Bochicchio, Miriam Jones and Eric Klein for field core collection and site photos, Daniel Brosseau for mapping assistance, and Michael Clifford for age modeling assistance. The work was supported by NSF-Ecosystem Studies Program (DEB-0919385).

TABLE OF CONTENTS

	Page
Title Page	i
Copyright Page	ii
Approval Page	iii
Acknowledgments	iv
Table of Contents	v
List of Tables	vii
List of Figures	viii
Abstract	1
Introduction	3
Research Question and Problem	3
Climate History Over the Last 15,000 Years	4
Peat Carbon Response to Paleoclimate Change	5
Study Objectives	6
Study Region and Site	7
Methods	9
Results	10
Lithology of Thermokarst and Permafrost Cores	10
AMS ^{14}C Dates and Core Chronology	11
Loss-on-ignition and C Accumulation Results	12
Macrofossil Analysis Results	13
Pollen Analysis Results	14
Grain Size Analysis Results	15
Discussion	16
Local Ecosystem and Environmental Change at the Study Site	16

Effects of Local Disturbances on Peatland Vegetation and C Accumulation……..…19

Rapid C Accumulation in Collapse Scar Fens………………………………………21

Neoglacial Cooling and Permafrost Aggradation in the Late Holocene……………..22

Conclusions and Implication……………………………………………………….….……….25

List of References……………………………………………..…………………………………..39

Biography……………………………..…………………………………………..……………………45

LIST OF TABLES

Page

Table 1: Lithology for core NL10-2…………..……………………………………………………..……27

Table 2: Lithology for core NL10-1……………..…………………………………………………..……27

Table 3: Radiocarbon dates from cores NL10-1 and NL10-2…………….………………………….28

Table 4: Results of grain size analysis at selected depths from core NL10-2………….……........29

LIST OF FIGURES

Page

Figure 1: Map and site information……………………………….…………………….…….30

Figure 2: Historical aerial photographs…………………………………….………………… 31

Figure 3: Climate data for Nome, Alaska………………….……………………….……………32

Figure 4: Age-depth model for non-permafrost core NL10-2.…………………………………..33

Figure 5: Age-depth model for permafrost core NL10-1………………….………………..……33

Figure 6: Summary macrofossil and LOI results from non-permafrost core NL10-2……………...34

Figure 7: Summary macrofossil and LOI results from permafrost core NL10-1…….……………..35

Figure 8: Pollen percentage diagram for core NL10-2……….………………………………………36

Figure 9: Pollen influx and concentration diagram for core NL10-2…………………………………37

Figure 10: Correlation diagram for the past 10,000 years……………..……………..……………..38

ABSTRACT

Northern peatlands have accumulated large carbon (C) stocks, acting as a long-term atmospheric C sink in the Holocene. However, how these C-rich ecosystems will respond to future climate change is still poorly understood. Furthermore, many northern peatlands are affected by permafrost, and it is challenging to project C balance under a changing climate and permafrost dynamics. In this study, we used a paleoecological approach to examine the effect of past climates and local disturbances on vegetation and C accumulation at a peatland complex on the Seward Peninsula, western Alaska over the past 13.5 ka (1 ka = 1000 cal yr BP). We analyzed two cores about 30 m apart, NL10-1 (from a permafrost peatland) and NL10-2 (from a non-permafrost peatland), for peat organic matter (OM) and C accumulation rates, macrofossil, pollen and grain sizes. Chronologies of the two cores were controlled by 6-14 accelerator mass spectrometry (AMS) ^{14}C dates on non-aquatic plant macrofossils.

The rapid C accumulation in the initial peatland at non-permafrost site NL10-2 from 13.5 to 12.8 ka and the presence of tree pollen from poplar (*Populus*) and spruce (*Picea*) indicate a warm regional climate, corresponding with the well-documented Bølling-Allerød warm period. Following a hiatus at 12.8-9.1 ka, high OM content (>80%), abundant *Sphagnum* and the presence of *Populus* pollen suggest high peatland productivity under a warm climate in the later part of the Holocene thermal maximum (HTM). Shortly after the HTM, a wet climate induced several major flood events at 8 ka, 6 ka, 5.4 ka, and 4.6 ka, as evidenced by decreases in OM, and increases in coarse sand abundance and aquatic fossils (algae *Chara* and water fleas *Daphnia*). Interestingly, there are no obvious changes in local plant communities, as rich fens dominated by brown mosses and sedges occurred from 8 to 4.5 ka. The initial peatland at permafrost site NL10-1 is characterized by rapid C accumulation (66 g C m^{-2} yr^{-1}), high OM content, and a peak in *Sphagnum* at 5.8-4.6 ka. A transition to extremely low C accumulation rates (6.3 g C m^{-2} yr^{-1}) after 4.5 ka at this site suggests the onset of permafrost, likely in response to Neoglacial climate cooling as documented across the circum-Arctic region. A similar decrease in C accumulation rates occurred at non-permafrost site NL10-2. Evidence from peat-core

analysis and historical aerial photographs shows an abrupt increase in *Sphagnum* and decrease in area of thermokarst lakes over the last century, suggesting major changes in hydrology and ecosystem structure, likely due to recent climate warming. The results from this study indicate that permafrost dynamics are controlled by both climate and site-specific factors, implying the difficulty in projecting responses of permafrost peatlands and their C dynamics to ongoing and future climate change.

1. Introduction

1.1. Research Question and Problem

Since the late 1950s, the overall global surface temperature has increased at a rate of 0.13°C per decade (IPCC, 2007). This change in average temperature has resulted in a decrease in snow cover by 10% since the late 1960s, widespread retreat of mountain glaciers, and a decrease in Northern Hemisphere spring and summer sea-ice extent by 10-15% since the 1950s (IPCC, 2007). The arctic system is particularly sensitive to climate warming due to the positive feedback effect of decreased albedo due to the melting of ice, snow and decreased sea-ice extent. Evidence of climate change in the arctic and sub-arctic has been well documented (Overpeck et al., 1997; Moritz et al., 2002), but the effects of this warming are not well understood in many arctic ecosystems.

Northern (boreal and subarctic) peatlands, many of which are underlain by permafrost, contain roughly one third of global soil carbon (C) – approximately 500 GtC in peatlands that has accumulated during the postglacial period (Gorham, 1991; Yu et al., 2010). The long-term ability of peatlands to sequester carbon dioxide from the atmosphere means that they play a critical role in modulating global climate (Turunen et al., 2001). High-latitude regions have been experiencing much greater warming than the global average in recent decades, which raises questions as to how these C-rich ecosystems will feed back to climate change. An additional concern in high latitude regions is how permafrost thaw (and thermokarst lake formation) will affect the global C balance. Permafrost occupies 22% of the exposed land surface of arctic and boreal regions in the northern hemisphere (Zhang et al., 1999), with an estimate of 277 GtC stored in permafrost peatlands (Schuur et al., 2009). These landscapes are highly dynamic and can change rapidly due to internal factors and/or climate (Jorgenson et al., 2001; Camill et al., 2001; Turetsky et al., 2002; Schuur et al., 2008; Tarnocai et al., 2009; Jones et al., 2012). Understanding how these ecosystems have responded to past climates and climate-induced disturbance is crucial for developing accurate climate and ecosystem models that are being used to project possible future changes.

1.2. Climate History Over the Last 15,000 Years

The Bølling-Allerød (BA) interstadial was a warm period that occurred from 14.7 to 12.7 ka, which represents the onset of deglacial warming in the northern hemisphere. Evidence in Alaska includes increased productivity in a lake in south-central Alaska coinciding with the BA warming (Yu et al., 2008), increases in thermokarst lake area (Walter et al., 2007), and expansion of peatlands (Jones and Yu, 2010). The initial deglacial warming of the BA was followed by a cold event known as the Younger Dryas (YD), a climatic reversal that occurred at 12.7 to 11.6 ka. While cooling during the YD is well documented, there are regional discrepancies in precipitation patterns across the northern high latitudes. While a dry YD characterizes eastern Siberia and interior Alaska, a wet YD characterizes Southern Alaska (Kokorowski et al., 2008; Mann et al., 2010; Kaufman et al., 2010).

The early Holocene was characterized by a warmer growing season across the boreal and arctic regions as a result of the response to maximum summer insolation at 11 ka caused by orbital cycles (Berger and Loutre, 1991). However, the timing of the Holocene Thermal Maximum (HTM) varies spatially throughout the arctic and subarctic due to regional factors, including deglacial history (IPCC, 2007). In Alaska, the HTM occurred at 11 to 8.5 ka, and was characterized by a decrease in sea-ice extent in the Arctic, a non-analog *Populus* forest/woodland in upland areas, high rates of peatland initiation and vertical C accumulation in lowland areas, and high rates of permafrost thaw (Kaufman et al., 2004; Edwards et al., 2005; Schuur et al., 2009; Jones and Yu, 2010; Mann et al., 2010).

In the mid-Holocene, glaciers began advances in association with Neoglacial cooling after 4.5 ka in sites throughout Alaska (Calkin et al., 1998; Levy et al., 2004). In addition, permafrost formation in much of the northern high latitudes after 4.5 ka was likely due to lower temperatures due to Neoglacial cooling (Peteet et al., 1998; Bauer and Vitt, 2011). More recently, the long-term cooling trend of the Neoglacial has been reversed due to 20th century warming (Kaufman et al., 2009). Air temperatures across Alaska have increased 1.3 °C in the past 50 years (Chapin et al., 2010) with rapid changes evident since the late 1970s (Hansen et al., 2006;

Osterkamp et al., 2009). While it is clear that the arctic is warming, the effect of these warmer temperatures on the permafrost and peatland C pools and the feedback potential of these ecosystems remain debated.

1.3. Peat Carbon Response to Climate Change

The balance of primary productivity and decomposition of the peatland control peat accumulation, with C sequestration occurring when primary production exceeds decomposition. Warmer temperatures stimulate peatland vegetation production, but can also increase decomposition rates. Whether peatlands will continue to act as C sinks under a warmer climate is highly debated (Roulet et al., 2007; McGuire et al., 2009; Beilman et al., 2010). During the warm HTM, northern peatland spread rapidly on the basis of >1500 basal peat dates (MacDonald et al., 2006), while vertical C accumulation rates in northern peatlands also show a peak during the HTM on the basis of 33 sites across the circum-arctic region (Yu et al., 2009). In addition, some peatlands in Alaska show increases in C sequestration during the Medieval Warm Period about 900 years ago (Hunt, 2010). These records indicate that peatlands are capable of increasing C sequestration under a warmer climate, but whether the net effect of C sequestration from peatlands coupled with CH_4 and old C release from thawing permafrost will lead to a negative feedback to climatic warming is highly debated (Schuur et al., 2009; Jones and Yu, 2010).

In the discontinuous permafrost zone, regional temperatures are not low enough to sustain permafrost everywhere, and as a result patterns of permafrost distribution are largely controlled by local factors such as topography, hydrology, vegetation, snow cover, and subsurface material properties (Schuur et al., 2008), which in turn affect C dynamics in these ecosystems. In permafrost landscapes, ground ice can occupy up to 80% of the soil volume, and thus thawing of ice-rich soils can trigger major changes in surface topography and ecosystem dynamics, including C release and uptake (Brown et al., 1998, Yershov, 1998; Schuur et al., 2008). Oftentimes, permafrost collapse leads to the formation of a thermokarst lake, which in turn can act as a positive feedback to permafrost thaw at the edges and bottom of the lake due to the higher heat capacity of water than air (Schuur et al., 2008). On the other hand, permafrost formation causes volume expansion of the freezing water, which raises the surface of a peatland well above the water table, thus creating drier conditions. At a fen-bog complex in northern Alberta, Canada, high accumulation rates in the early Holocene declined markedly after 4 ka due to permafrost aggradation (Bauer and Vitt, 2011). If surface conditions become too dry, peat accumulation can cease, since oxidation of the surface peat increases (Vitt et al., 1994). However, there may be little difference in NPP before and after permafrost thaw due to tradeoffs between long-term woody tissue growth on permafrost plateaus and rapid moss growth in permafrost collapse areas (Camill et al., 2001).

In addition to how permafrost thaw and aggradation affect peatlands, many experimental peatland studies have investigated how changes in moisture can affect peat C dynamics and vegetation change, specifically focused on how a higher water table caused by flooding might affect peatland ecosystems (Camill et al., 2001; Churchill, 2011). Long-term flooding kills terrestrial plants, removing that C sink potential, and also causes enhanced emissions of C greenhouse gases (Kelly et al., 1997; St. Louis et al., 2000). Alternatively, short-term flood events lead to an increase in aboveground NPP and little affects on the peatland vegetation (Churchill, 2011). In a study in Poland, flooding by a river delivers important nutrients (K, Ca) to the peatland that stimulate productivity, but can also stimulate decomposition (Wassen et al., 1990). Another study from Quebec, Canada suggests peatland flooding may have caused tree and woody shrub mortality, and that repetitive flooding was an important process controlling peatland development (Bhiry et al., 2007).

1.4. Study Objectives

The objectives of this study were to derive a multiple proxy record of ecosystem change in order to gain understanding of controls on C accumulation in peatlands and to gain insight into how climatic changes and disturbance affect peatland ecosystem dynamics. One aspect of understanding how these high-latitude ecosystems have responded to past climates is having a spatially variable, high-resolution dataset from regions of variable climates (temperature, precipitation, humidity, etc.) and local factors (topography, aspect, vegetation type, etc.) so it is possible to realize the controlling factors of C accumulation and ecosystem change in peatlands within and across various climatic gradients. C accumulation histories of some regions in the arctic and subarctic have been well researched, while other, more remote locations, remain poorly understood. Within Alaska, the southern Seward Peninsula has no peat C accumulation records. This region is of particular interest due to its location near the forest-tundra ecotone and location within the discontinuous permafrost zone, which makes it sensitive to climate change. Furthermore, this is a region close to the Bering Sea, so there is the potential for this region to respond sensitively to sea-ice extent, which is expected to decrease with a warmer climate. Therefore, a high-resolution record of ecosystem change and C accumulation from this region would provide a valuable dataset for large-scale synthesis of climate and ecosystem change at regional and Pan-Arctic scales and for understanding the importance of climate and moisture variability on hydrological and ecosystem processes in the recent past.

2. Study Region and Site

The study region is on the southern Seward Peninsula, western Alaska (Figure 1A). The glacial history of the Seward Peninsula is limited to the small glaciers of the Kigluaik Mountains, which lie ~80 km northwest of the study site. The glaciers have displayed typical recession during recent warming and moraine evidence for the Little Ice Age (Calkin et al., 1998). The study area appears to be an old or possibly current floodplain of the Niukluk River, and is currently located near the confluence of the Niukluk and Fish rivers (Figure 1B), but lies at the border of two drainage basins: the eastern basin drains approximately 3279.96 km^2 while the western basin drains approximately 2304.57 km^2 (Figure 1B). In addition, the study region is in the discontinuous permafrost zone (Figure 2); therefore, permafrost dynamics exert a strong control on local hydrology.

The study region experiences a maritime climate that is controlled by the Bering Sea and sea surface conditions (especially sea-ice extent). The closest weather station to the study region is located in Nome, AK, which is about 100 km southwest of the site. The mean annual temperature (MAT) in Nome is -2.74° C, mean annual precipitation is 420.6 mm and mean annual snow depth is 1.45 m for the period 1971-2000 (NOAA; Figure 3). The area around the study region supports both tundra and forest vegetation types. Lichen-dominated tussock tundra is abundant in the lowland areas, which are heavily influenced by permafrost. Forests dominated by *Picea* and *Larix* occur in the upland areas (Hinzman et al., 2005). In addition, the study region is located near present-day treeline (CAFF, 2001), and therefore, this is well positioned to show treeline shifts during past climatic changes or species migrations.

Two study sites are located near Niukluk Lake (unofficial name; Figure 1D and Figure 2). Site NL10-2 is from a non-permafrost peatland at the edge of Niukluk Lake below a nearby permafrost peat plateau (coring site: 64° 49.645' N, 163° 27.235' W; elevation = 16 m asl; Figure 1C). Site NL10-1 is located on the permafrost plateau (coring site: 64°49.648' N, 163° 27.265' W; elevation = 18 m asl; Figure 1C); which is about 2 m above coring site NL10-2. The active layer depth of coring site NL10-1 was 63 cm in August 2010. These two sites are located about 30 m apart. These coring sites are near the border of two drainage basins but technically lie within the eastern basin of the Fish River, but are closer to the Niukluk River. Therefore, the Niukluk River and potentially the Fish River present possible strong local influences on the peatland study sites, particularly core NL10-2, which is only 500 meters from the nearest river meander of the Niukluk River and only 4 meters in elevation above the river. In addition, the study sites are within a fluvial floodplain underlain by marine alluvium (Statewide Alaska Geology, 1999), which could potentially be a source of carbonate to the peatland through groundwater transport.

Historical aerial photos of the site dating back to 1950 show major changes in the study region over the past 60 years (Figure 2). It appears that portions of Niukluk Lake have expanded into the permafrost plateau (lower left portion of the lake) owing likely to permafrost thaw and retreat of permafrost edge, while the floating peat mat has expanded over parts of the lake (center of lake; upper portion of lake). Also, some thermokarst lakes visible in the 1950 and 1980 photographs west of Niukluk Lake (two lakes) and north of Niukluk Lake are vegetated in the 2009 photograph. This series of images displays the complex nature of landscapes affected by thermokarsting and the relatively rapid changes that can occur in this ecosystem due to local factors.

3. Methods

Core NL10-2 (272-cm in length) was collected from the non-permafrost peatland (thermokarst) site near Niukluk Lake using a Russian-type peat corer, while core NL10-1 (293-cm in length) was collected from the peat plateau site using a Laval permafrost corer (Calmels et al., 2005), both in the summer of 2010 (Figure 1C). Core NL10-2 was wrapped in plastic films, stored in half PVC pipes, and transported to the laboratory at Lehigh University. The core was sectioned in the laboratory into continuous 1-cm slices for loss-on-ignition, macrofossil, and pollen analysis. Core NL10-1 was sectioned in the field into 2.5-cm-long sections for the non-frozen portion (top 63 cm active layer) of the core and ~10-cm-long sections for the frozen portion (63-293 cm). Core NL10-2 was used for most of the analysis, while core NL10-1 was used for dating, loss-on-ignition and macrofossil analysis at coarse sampling resolution.

Fourteen accelerator mass spectrometry (AMS) ^{14}C dates were obtained from core NL10-2, and six from core NL10-1. Non-aquatic macrofossil species were selected for dating, with *Sphagnum* remains being selected when possible. Samples were cleaned at Lehigh University and measured for ^{14}C at the University of California Irvine KECK Carbon Cycle AMS Laboratory. Age-depth models were derived from the Clam “classic” age-depth modeling program (Blaauw, 2010; Figures 4 and 5). In the process, the ^{14}C dates are calibrated (Reimer et al., 2009; Stuiver and Reimer, 1993), and age-depth curves are constructed based on linear interpolations. For each date, the probability of a calendar year being sampled is proportionate to its calibrated probability. Uncertainty ranges as well as a 'best' age-model are calculated. Calibrated radiocarbon ages fitted to these age-models were then used to estimate sedimentation rates and C accumulation rates for both cores.

Loss-on-ignition was performed on both cores to estimate organic matter (OM) content and bulk density. For each sample, 1 cm^3 of sediment was dried at 100°C overnight, weighed, and combusted at 550˚ C for 1 hour, and weighed again. Organic matter content and ash-free bulk density were used to estimate C content of the cores and C accumulation rates. Macrofossil analysis was completed, on average, every 2-cm for NL10-2 and every 4-cm for NL10-1 by sieving a 1-cm^3 sample through a 250-μm sieve and identifying peat remains using a binocular microscope.

Pollen analysis was completed for core NL10-2 at approximately 4-cm intervals, using 1-cm^3 sediment subsamples. Pollen processing followed the standard procedure (Faegri and Iversen, 1989). Sieving was used to remove fine and coarse materials. A known number of *Lycopodium clavatum* spores were initially added to each sample as a spike for calculations of pollen concentration (batch no. 938934). Samples were then mounted onto glass slides with silicon oil and identified and counted under a compound microscope for pollen.

Grain size analysis was completed for five selected intervals with high mineral content in core NL10-2. At least 1 g of sediment was placed in a beaker with 30% H_2O_2, and then placed in a hot water bath until the reaction ceased (about a half hour). Once all OM was digested, samples were transferred to centrifuge tubes and centrifuged for 35 minutes. Samples were then decanted, rinsed with water, mixed, and then centrifuged for an additional 35 minutes. Samples were then transferred to Petri dishes and placed in a drying oven for 24 hours. Once dry, samples were broken up with a mortar and pestle and put through the Dual Manufacturing Co. U.S. standard testing sieve series. Each size fraction was weighed and percent of sample for each size fraction was calculated.

4. Results

4.1. Lithology of Non-Permafrost and Permafrost Cores

The 272-cm peat core from thermokarst site (core NL10-2) was collected in 6 drives of 50 cm in length each with drive connection at 50 and 100 cm depth, plus an additional 25-cm thick monolith to cover the gap in the top loose peat. The base of the core is gray sand and coarse quartz sand (Table 1). From 274-190 cm, the core is brown, peaty organic sediments intermixed with some gray silt-rich layers. There is a sharp contact in the record at 190 cm. From 190-144 cm, the sediment changes to more organic-rich peat, although there are still some silt-rich layers (Table 1). From 144-117 cm, the lithology is gray, silty, humified peat. From 117 cm onwards, a well-preserved, sedge peat persists to the top of the core. However, there is a gap in the record from 50-40 cm due to problems during core extraction.

The 293-cm peat core from the permafrost site (core NL10-1) was collected in 13 drives of varying length. The base of the core is sandy with shells and some organic silt, which persists until 266 cm (Table 2). From 266 to 232 cm the material is more organic, with much less silt. At 232 cm, there is a transition to ice-rich, organic peat in a silt/sand matrix, which persists until 125 cm (Table 2). From 125-63 cm, the lithology is well-preserved peat with ice lenses at some intervals. The top 63 cm of this record was very well preserved, dense peat free of ice.

4.2. AMS ^{14}C Dates and Core Chronology

The dating results from both cores are shown in Table 3. For core NL10-2, among the fourteen dates analyzed, three dates at 62, 160, and 172 cm were rejected. The too old date at 62 cm was rejected due to an age reversal, which is most likely due to dating of selected brown moss stems, which can take up old C (Table 3). The dates at 160 and 172 cm are also too old and with large errors, likely due to dating multiple macrofossil types (Table 3). Also, it is possible that the material may have been washed in during disturbance events (see below for discussion of flooding events near those dates). The age-depth model for core NL10-2 (Figure 4) is based on linear interpolation using Clam between the 11 remaining calibrated ages for two intervals before (13.5-12.8 ka) and after the hiatus (9.1 ka to present). The sedimentation rate is highest (0.09 cm/yr) from 13.5 ka to 12.8 ka (at 258-193 cm). Following this rapid sedimentation, a sedimentation hiatus occurred at 12.8-9.1 ka (193-188 cm). During the last 9 ka, the sedimentation rate is 0.02 cm/yr on average.

For core NL10-1, the date at 7.5-10 cm was labeled as an outlier before running the data through Clam due to an age reversal between 7.5-10 cm and 26-28.5 cm (Table 3). There is no strong justification for rejecting either of the dates at those depths, so we acknowledge the dating uncertainty in this core for the last 4.5 ka. We based our decision off of the Clam output, which labeled the age-model rejecting the date at 7.5-10 cm a much better fit than the age-model rejecting the date at 26-28.5 cm. The age-model for core NL10-1 (Figure 5) is based on linear interpolation using Clam between the 5 remaining calibrated ages. Starting at the base of the core, sedimentation is extremely rapid (0.46 cm/yr) between 6.4 and 6.2 ka (218-144 cm). Following this section, sedimentation rate slows down to 0.07 cm/yr at 6.2 to 4.5 ka (139-126 cm). At 4.5 ka, sedimentation rate decreases by an order of magnitude to 0.008 cm/yr. From 2 ka to present the sedimentation rate is the lowest for the whole core at 0.002 cm/yr.

4.3. Loss-on-Ignition and C Accumulation Results

The average OM content for core NL10-2 is 44% (Figure 6). The OM content shows a general long-term increasing trend from <6% at the base (13.7 ka) to >90% (present). In addition to this long-term trend, there are multi-millennial oscillations in OM content between ~20% and ~80%. OM content is low at 13.5-12.8 ka, with an average of 15.7% OM. After the hiatus from 12.8-9.1 ka, OM content increased to ~80% at 9 ka but then decreases steadily to a low value of 20% by 8 ka. There are three additional low OM intervals at 6 ka, 5.4 ka, and 4.6 ka. From 4.5 ka to present, OM increases steadily from <40% to >95%.

The average ash-free bulk density for core NL10-2 is 0.16 g/cm^3. From 13.5 to 12.8 ka, ash-free bulk density is fairly steady with an average of 0.15 g/cm^3. Ash-free bulk density shows a general increasing trend from ~0.17 g/cm^3 at 9.1 ka to 0.22 g/cm^3 at 6.5 ka. Ash-free bulk density then shows a general decreasing trend from 6.5 ka to present. The average time-weighted C accumulation over the entire record for core NL10-2 is 21.2 g C m^{-2} yr^{-1}. The bottom section of peat has the highest C accumulation at an average of 71 g C m^{-2} yr^{-1} at 13.5-12.8 ka, followed by the hiatus at 12.8-9.1 ka. The C accumulation rates show a general increasing trend from 10 g C m^{-2} yr^{-1} at 9.1 ka to 30 g C m^{-2} yr^{-1} by 4.8 ka. After 4.8 ka, C accumulation steadily decreases to 5.2 g C m^{-2} yr^{-1} at ~1.3 ka, after which C accumulation increases to an average of 46.4 g C m^{-2} yr^{-1} by 1870 C.E.

For core NL10-1, the average OM content is 48% (Figure 7). The OM content is low at the base of the core (average of 23% OM), but increases to 90% OM at 5.7 ka. At 4.8 ka, there is a decrease in OM content to 18%, after which OM shows a general increasing trend to 73% at the top of the core. The average ash-free bulk density for core NL10-1 is 0.14 g/cm^3. Ash-free bulk density is relatively stable from 6.5 to 5.7 ka with an average of 0.11 g/cm^3. From 5.7 ka to present, ash-free bulk density becomes more variable, with a range from 0.04 to 0.24 g/cm^3 and an average of 0.14 g/cm^3.

The average time-weighted C accumulation in core NL10-1 is 21.8 g C m^{-2} yr^{-1}. Extremely rapid C accumulation characterizes this core at 6.5-6.2 ka, with an average of 316 g C m^{-2} yr^{-1}. At 6.2 ka, C accumulation drops to an average of 28 g C m^{-2} yr^{-1} until 5.4 ka, at which point C accumulation more than doubles to an average of 69 g C m^{-2} yr^{-1}. From 4.9 ka to present, C accumulation is extremely low at an average of 3.6 g C m^{-2} yr^{-1}. However, there is uncertainty in these values during this time period due to poor chronological controls.

4.4. Macrofossil Analysis Results

Macrofossil zones in core NL10-2 have been identified with the aid of CONISS cluster analysis and plotted with the Tilia software, version 1.7.16 (Figure 6; Grimm, 1992). Zone M2-1 (13.5-12.8 ka) is dominated by brown mosses and woody material. The base of this zone is characterized by high percentages of brown mosses (mostly *Drepanocladus*), sedges and *Sphagnum,* followed by a large increase in woody material at 13.3 ka. By 13.05 ka woody material decrease and brown moss and *Sphagnum* increase along with the amount of mineral material and aquatic species present in the core. A hiatus occurs from 12.8 to 9.1 ka.

The dominant vegetation in zone M2-2 (9.1-4.5 ka) is sedge. This zone is divided into two subzones (M2-2a and M2-2b; Figure 6) the first of which begins after the hiatus at 9.1 ka with a dominance by *Sphagnum* and the absence of mineral material or aquatic fossils. By 8.7 ka *Sphagnum* decreases from >60% to <40% followed by an increase in brown mosses, woody material, coarse mineral material (>250 μm) and aquatic fossils. There is a major increase in mineral content from ~10% to >20% at 8 ka. Subzone M2-2b begins at 7 ka when all moss species decrease or disappear, mineral material is absent, and sedge dominates the ecosystem. At 6 ka, there is a second peak of mineral material, which is identified by the increase in coarse mineral content from 0% to 30%. Sedge percentages drop and mosses re-appear synchronously with the increase in mineral material. Two more peaks in mineral content occur at 5.4 ka and 4.6 ka, but the macrofossils remain relatively stable through the remainder of this zone.

Zone M2-3 (4.5-0.05 ka) is dominated by sedge. This zone is characterized by the disappearance of mineral material and aquatic species. Sedge content is high throughout this zone (~65%), while woody material, brown mosses, and *Sphagnum* occur in nearly equal abundance. Towards the top of this zone, there is change in dominance from sedge, to woody material, and then finally to brown mosses. The most recent Zone M2-4 (1900-2010 C.E) is characterized by an increase in *Sphagnum* to nearly 100% as other macrofossil types all but disappear.

Permafrost core NL10-1 was divided into 4 zones and plotted with the Tilia software, version 1.7.16 (Figure 7; Grimm, 1992). The dominant macrofossils in zone M1-1 (6.5-5.9 ka) are woody material, sedge, and brown mosses. Also, this zone is characterized by the presence of mineral material and aquatic species. Zone M1-2 (5.9-4.6 ka) is characterized by the dominance of *Sphagnum*. Sedges are also dominant in this zone. Following a peak in *Sphagnum* of 80% at 5.5 ka, *Sphagnum* decreases and sedges begin to dominate. The dominant vegetation types in zone M1-3 (4.6-2.5 ka) are sedges and woody material, with the beginning of the zone being dominated by sedges and the end of the zone being dominated by woody material. *Sphagnum* is absent during this zone, while brown mosses are absent for the majority of this zone but reappears by 3.1 ka. Zone M1-4 (2.5 ka to present) is characterized by the dominance of woody material.

4.5. Pollen Analysis Results

Pollen zones have been identified with the aid of CONISS cluster analysis and plotted with the Tilia software, version 1.7.16 (Figure 8; Grimm, 1987; Grimm, 1992). Pollen concentration, pollen influx, and *Picea* influx were also calculated and are shown in Figure 9. In zone P-1 (13.5-12.8 ka), the dominant taxa are *Betula, Salix,* and Poaceae, suggesting shrub tundra with rapid pollen influx rates. Sub-zone P-1a is characterized by the presence of *Picea, Larix* and *Alnus* pollen, indicating a shrub-tundra possibly with scattered trees or treed islands. In sub-zone P-1b (13.2-13.08 ka), these pollen types disappear, indicating a transition to herb tundra. In sub-zone P-1c (13.08-12.8 ka), *Betula* increases and *Populus* migrates into the area, indicating a transition from herb tundra to woodland/deciduous forest, which is accompanied by an increase in pollen influx rates from the previous sub-zone. The dominant taxa in zone P-2 (9.1-8.1 ka) are *Betula* and Poaceae, with the presence of *Populus* pollen, indicating a woodland/deciduous forest. The dominant taxon in Zone P-3 (8.1-4.8 ka) is *Betula.* The first subzone, P-3a (8.1-7 ka; Figure 8), is characterized by a dominance of *Betula* and high percentages of Poaceae, suggesting a shrub/herb-tundra environment. Sub-zone P-3b is characterized by the reappearance of *Picea* and *Alnus,* an increase in Ericaceae, and a decrease in Poaceae, suggesting a transition to a more forested ecosystem. Subzone P-3c is characterized by a return to shrub tundra, as suggested by the significant decreases in *Picea* and *Alnus* and an increase in *Betula*. The dominant taxa in zone P-4 (4.8-2.5 ka) are *Alnus* and *Betula.* This zone characterized by an increase in *Picea* and *Alnus* towards the top of this zone (Figure 8) and major decreases in *Betula* pollen and *Sphagnum* spores, indicating an increase in regional forestation. The dominant taxa in zone P-5 (2.5 ka to present) are *Picea* and *Alnus.* This zone is differentiated by increasing percentages of *Picea, Larix, Betula,* and *Alnus* and a decrease in Poaceae and Cyperaceae toward the top of the core, indicating the expansion of forests in this region.

The late Holocene increase in *Picea* pollen may represent the increase of black spruce (*Picea mariana*) trees, because of progressive increases in moisture and paludification on the forest floors. This has been documented in Western Alaska (Anderson and Brubaker, 1994; Lozhkin et al., 2011). However, we did not separate *Picea* pollen in this study.

4.6. Grain Size Analysis Results

Grain size analysis results on five samples from the various flood events are shown in Table 4. All samples have a bimodal distribution, with a peak in the very fine sand/silt size fraction (<63 μm) and a peak in the fine sand/medium sand size fraction (150-200 μm). The disturbance events at 100 cm (4.6 ka) and 130 cm (6 ka) have a larger proportion of grain sizes greater than 125 μm than the other events, possibly indicating a greater magnitude of disturbance.

5. Discussion

5.1. Local Ecosystem and Environmental Change at the Study Site

Peat began accumulating at the non-permafrost (thermokarst) site by 13.5 ka on coarse sand and gravels during the Bølling-Allerød interstadial (BA), a known warm period from 14.7 to 12.7 ka (Figure 6; Kokorowski et al., 2008; Kaufman et al., 2010). The very high C accumulation rate (71 g C m^{-2} yr^{-1}) at 13.5 to 12.8 ka was likely a response to early deglacial warming during the BA period. Pollen results showing an abundance of *Salix* and *Betula* during the BA suggest shrub tundra, likely with scatted trees (*Picea* and *Larix*) around the peatland. Additionally, high pollen concentrations and influx rates also suggest high productivity in this region (Figure 9). Locally, the peatland began as a rich fen dominated by *Sphagnum*, brown mosses, and sedges. A major transition at 13.3 ka (240 cm) to increased woody material and decreased sedge and bryophytes resulted in slightly decreased OM content that are likely due to a brief dry and cool climate interval, which is corroborated by an increase in Poaceae and disappearance of *Picea* and *Larix* in the pollen record. These changes could be due to a brief cold period known as the Intra-Allerød cold period (~13.3 ka; Donnelly et al., 2004) that may have resulted in increased sea-ice in the Bering Sea and cooler sea-surface temperatures.

A return to a wetter local climate is apparent at 13.1 ka (225 cm), as indicated by a decrease in woody material and an increase in *Sphagnum*, brown mosses, and aquatic fossils (*Chara* and *Daphnia*). Also notable, this record indicates the expansion of *Populus* into this area at about 13.1 ka, which is in agreement with other records in the region (Mann et al., 2010). In addition, this interval from 13.1 to 12.8 ka has a steadily increasing amount of mineral material inundating the site, with a maximum of 50% of sediment being mineral with the majority of the grain sizes being fine silt/clay from grain size analysis (Table 4). This could be due to potential slumping in of mineral soil as the thermokarst lake expands, or possibly due to flooding of the nearby Niukluk River or its tributaries. A return to wetter and warmer regional conditions in lowlands is indicated by an increase in *Betula* and Ericaceae and disappearance of Poaceae. This shift to a more mesic climate may be due to reduced sea-ice in the Bering Sea and northwest Pacific Ocean in addition to warmer sea surface and air temperatures, which would have allowed more moisture to evaporate and to be transported to eastern Beringia (Ager, 2003).

The BA was followed by the cold, and possibly dry Younger Dryas event, which spanned from 12.7 to 11.6 ka (Kokorowski et al., 2008). Results from this study show a hiatus at 12.8-9.1 ka, spanning the entire YD interval. This hiatus could be partly due to drying during the YD (Peteet and Mann, 1994; Hu et al., 2002; Axford and Kaufman, 2004). Alternatively, the hiatus occurring right before an increase in OM from <20% to >80% and a major change in lithology suggests that sometime between 12.8 and 9.1 ka the site was a thermokarst lake and that it rapidly, catastrophically drained, scouring sediments along with it. Studies indicate that thermokarst lakes formed frequently during the Holocene thermal maximum (HTM; 11-8.5 ka; Côte and Burn, 2002; Walter et al., 2007), and that lateral expansion of thermokarst lakes can lead to gradual or catastrophic drainage (Hinkel et al., 2007; Jones et al., 2012). Additionally, in Siberia and Alaska the frequency of thermokarst basin formation shows a major peak at 10.5 ka (Walter et al., 2007; Mann et al., 2010).

The HTM period at 9.1-8.5 ka is not well represented at this site due to the sedimentary hiatus in the record. However, high OM content and *Sphagnum* dominance directly following the hiatus suggests a productive poor fen, while the presence of *Populus* in the pollen record indicates a warm and possibly dry climate (Figure 9). These results are in agreement with studies that indicate a non-analog *Populus* forest in upland areas, and a high frequency of peatland initiation (Kaufman et al., 2004; Edwards et al., 2005; Mann et al., 2010; Jones and Yu, 2010), which were possibly due to decreased sea-ice extent during the HTM owing to maximum summer insolation (Berger and Loutre, 1991).

Pollen data from core NL10-2 suggest a regional dominance by *Betula* (45%) throughout the mid-Holocene (8.5-4.5 ka), suggesting a shrub-tundra ecosystem. Disappearance of *Populus* from the record at 8 ka suggests a return to cooler conditions, possibly influenced by rising sea levels (Davies et al., 2011) and expanded sea ice in nearby Bering Sea following the gradual decline in summer insolation. Despite a large local flooding event at 8 ka (see discussion below), which caused a decrease in OM content from 50% to 20% at site NL10-2, there was little or no recorded effect on the peatland vegetation community. Sedge and mosses (*Sphagnum* and brown mosses) dominated from 8.5 to 7.5 ka, suggesting wet but surprisingly stable ecosystem conditions. Pollen and macrofossil evidence suggests wet lowlands, likely caused by increased precipitation owing to increased moisture availability in a more maritime climate as a result of a high sea level. Studies throughout Alaska indicate rising lake levels and increased soil moisture starting ~9 ka (Carter, 1993; Abbott et al., 2010; Edwards et al., 2001; Mann et al., 2002a), perhaps influenced by a cool climate after the HTM and a rising sea level. Effective moisture continued to increase in Alaska until ~5.5 ka (Hu et al., 1998; Axford, 2000; Edwards et al., 2001), possibly also increasing winter snowfall. Records throughout Alaska indicate an abrupt expansion of *Alnus crispa* at ~7 ka (Wright and Porter, 1984; Anderson and Brubaker, 1994; Cwynar and Spear, 1995; Hu et al., 2001; Ager, 2003; Axford and Kaufman, 2004). This record indicates migration of *Alnus* into the region at about 7 ka, but it did not reach its modern abundance in this region until 4.5 ka. It is possible that an increase in winter snowfall favored *Betula* expansion between 6 and 4.5 ka.

Locally, macrofossil results from core NL10-2 suggest a transition to more stable conditions at 7 ka as mineral material disappears from the record and sedges dominate, suggesting an extreme rich fen with no disturbances. The macrofossil and LOI record from core NL10-1 begins at 6.5 ka and suggest rapid C accumulation (296 g C m^{-2} yr^{-1}) and sedimentation likely in a collapse scar fen. Dominance by sedge, brown mosses, and presence of aquatic algae *Chara* at NL10-1 at 6.5 ka also suggests wet local lowland conditions. Carbon accumulation decreases at site NL10-1 at 6.25 ka from 296 g C m^{-2} yr^{-1} to 28 g C m^{-2} yr^{-1}, which suggests a major ecosystem shift, likely due to autogenic peat growth above the water table and unrelated to regional climate, as the pollen record suggests no major changes in regional vegetation at that time. Alternatively, the very high C accumulation rates at 6.5-6.25 ka may be an artifact of dating uncertainty or errors of these two bracket dates. In core NL10-2, LOI and macrofossil results indicate a major disturbance at 6 ka: a sustained decrease in OM content to 30% and an increase of mineral material occurs contemporaneously with a decrease in sedges from >80% to <50%, and a reappearance of both *Sphagnum* and brown mosses. Two additional discrete flood events occurred at this site at 5.4 ka and again at 4.6 ka, but both result in little noticeable vegetation changes (see next subsection for more discussion on flooding disturbances).

Beginning at 4.5 ka, there is a major shift in the pollen record with a decrease in *Betula* from 45% to <20% and an increase in *Alnus* from 10% to 30%. In addition, Poaceae increases from 5% to 25%, *Picea* pollen reappears, and there is a significant decrease in *Sphagnum* spores. Increased forest cover likely elevated evapotranspiration in this region, acting as a positive feedback to depleting soil moisture and possibly preventing flooding. At site NL10-2, a disappearance of flooding evidence and aquatic fossils occurs at 4.5 ka, which also suggests a shift to drier conditions. In core NL10-1, *Sphagnum* and brown mosses disappear at 4.6 ka, which coincides with a major decrease in OM from >80% to <20%, suggesting a major ecosystem shift at this site, possibly due to permafrost aggradation. Additionally, the gradual increase in ash-free bulk density and woody material from 4.5 ka to present suggests a high peat decomposition and poor preservation, likely caused by the aggradation of permafrost, although poor dating control limits our ability to identify the more precise timing of permafrost aggradation. At site NL10-2, the lack of local disturbances following 4.5 ka likely allows the peatland to thrive, as evidence by increasing OM and an increase in *Sphagnum.* However, there is a general decreasing trend in C accumulation at site NL10-2 between 4.5 and 0.1 ka, owing possibly to a drier/cooler climate. Rapid C accumulation and fresh, well-preserved plant tissues prevail in the acrotelm (the top 20 cm), and changes in vegetation likely indicates autogenic succession from a brown moss and sedge dominated rich fen to a *Sphagnum*-dominated poor fen over the last 100 years.

5.2. Effects of Local Disturbances on Peatland Vegetation and Carbon Accumulation

A prominent feature of this record is the multiple millennial-scale oscillations in OM content during the mid-Holocene (Figure 10A). Four discrete flood events have been identified in this record at 8 ka, 6 ka, 5.4 ka, and 4.6 ka. One possibility is the flooding of the Niukluk River or its smaller tributary rivers that flow from the hills/mountains less than 4 km north of the study site. Grain size analysis of the flood intervals suggests a range of grain sizes from clay to medium sand grains, with a peak in the clay and 150-250 μm size fractions, with grains as large as 500 μm being deposited at these intervals (Table 4). Increased precipitation starting ~9 ka may have contributed to the flooding of rivers around this site (Carter, 1993; Abbott et al., 2010; Edwards et al., 2001; Mann et al., 2002a; Lozhkin et al., 2011). Additionally, enhanced winter storminess and increased snowfall (Mann et al., 2002b) would increase spring melt and possibly increase flooding at this site as well. The scenario of increasing snowfall seems to be consistent with increase in *Betula* pollen during this time interval. It is also possible that regional precipitation started to decrease around 4.8 ka, likely due to the weakening of the Pacific Subtropical high, which would result in fewer storms reaching NW Alaska (Mann et al., 2002b). These changes in atmospheric circulation likely contributed to regional drying around 4.5 ka, which coincides with the disappearance of flood events from the study site. Further evidence for flooding is the lack of observable changes in macrofossils at core NL10-2 with the flood events: peatlands are known to be resilient following short-term flood disturbances (Camill et al., 2001; Churchill, 2011).

Alternatively, these flood events could be explained by permafrost dynamics around coring site. A wetter/mild climate may have enhanced permafrost thaw around the edges of Niukluk Lake, which might cause enhanced drainage from nearby ice-rich mineral soils into the peatland (Jorgenson et al., 2001; Turetsky et al., 2002; O'Donnell et al., 2012). Fungal Sclerotia found at 3 out of the 4 flooding intervals suggest influx from mineral soils, more likely from nearby upland than by rivers. There are instances of thermokarst lake formation in the Arctic during this time period (Walter et al., 2007; Brosius et al., 2012); however, there is no evidence suggesting that permafrost existed at this site during this time interval. Therefore, further study is needed in this area to determine if permafrost existed at this site prior to 4.5 ka.

Carbon accumulation rates at site NL10-2 appear to remain stable throughout and after all of the disturbance events at an average of 19 g C m^{-2} yr^{-1}; however, the OM content is extremely variable from 8 ka to 4.5 ka. The less variable C accumulation rates could be caused by the lack of adequate dating to bracket individual flooding events. Meanwhile in core NL10-1, the 6 ka event coincides with a major decrease in OM content from 50% to 20% and the appearance of mineral material in the core. Directly following the 6 ka event, OM content abruptly increases from <30% to >90% (Figure 10B). The macrofossil results from this core suggest classic autogenic succession of peatland vegetation from rich fen to poor fen and possibly to bog as the peatland gradually grows higher and further away from the water table (Figure 10C). It is not clear how or if the successional changes on the peatland are related to the disturbance event, although it is possible that flooding would deliver nutrients to the system, which might enhance productivity and peatland growth (Wassen et al., 1990).

The 5.4 ka event in core NL10-2 coincides with a major increase in *Sphagnum* and disappearance of mineral and aquatic species in core NL10-1 (Figure 10C). Additionally, the 4.6 ka event coincides with a sudden disappearance of *Sphagnum* and increase in sedges at NL10-1 (Figure 10C). These major events and changes occurring concurrently in both records suggest that these two sites are hydrologically connected and respond to the same disturbances, although possibly in very different manners. While OM decreases suddenly with each disturbance event at site NL10-2, there are few observable changes in the macrofossil record. However, at site NL10-1 the disturbance events at 6 ka and 4.6 ka as documented at site NL10-2 coincide with major decreases in OM content and major changes in the macrofossil record; Additionally, a lack of sand-sized grains suggests finer mineral material was deposited at this site than at NL10-2. This suggests that peatlands at site NL10-1 may be more sensitive to flooding than site NL10-2, either because of different preexisting vegetation or possibly due to fine mineral particles having large impacts on peatland vegetation. Additionally, grain size analysis results from core NL10-2 for the 6 ka and 4.6 ka events show an increase in the percentages of sand grains greater than 125 μm for these two events compared to other events (Table 4), suggesting that the magnitude of the disturbance was greater at 6 ka and 4.6 ka than the other events.

5.3. Rapid Carbon Accumulation in Collapse Scar Fens

The effects of permafrost thaw on the C balance of high-latitude peatlands remains a key uncertainty in our capacity to assess the effects on the global climate system. Both sites experience periods of extremely rapid accumulation at the beginning of their depositional history, owing possibly to the formation of collapse scar fens following the initial postglacial permafrost degradation at these sites. However, the lithology at the base of core NL10-2 appears to be fluvial sands and gravels, suggesting that it may have never been permafrost. During the BA, NL10-2 experienced rapid sedimentation with C accumulation rates of 71 g C m^{-2} yr^{-1}, which may be either owing to increased plant productivity under a warm climate or an autogenic process typical of collapse scar fens (Roulet et al., 2007; O'Donnell et al., 2012). It is possible that warmth during the BA contributed to the collapse of remnant permafrost from the last ice age; an increase in thermokarst initiation around 13.5 ka from a large data synthesis across circum-Arctic region corroborates this idea (Walter et al., 2007). At site NL10-1, it appears that permafrost collapsed before 6.5 ka (possibly triggered by flooding), with an average C accumulation rate of 296 g C m^{-2} yr^{-1} from 6.5 to 6.35 ka, which is extremely rapid even for collapse scar fens. However, this rate calculation relies on the reliability of two bracketed ^{14}C dates. These C accumulation rates are high compared to a synthesis of northern peatlands (18.6 g C m^{-2} yr^{-1}; Yu et al., 2009), but the rate of 71 g C m^{-2} yr^{-1} at core NL10-2 is similar to C accumulation rates in collapse scar fens in Interior Alaska (61 g C m^{-2} yr^{-1}; O'Donnell et al., 2012).

The question remains as to whether the C accumulation following permafrost collapse is greater than the C loss that occurs in the forms of methane and old C as more material becomes available for decomposition. Results from the Koyukuk National Wildlife Refuges in central Alaska suggest that organic C loss following permafrost thaw is greater than subsequent peat C accumulation (O'Donnell et al., 2012). In addition, formation of a collapse scar fen is a positive feedback that accelerates permafrost thaw (Davies et al., 2012), which can lead to greater C loss as thawing organic material becomes available for decomposition. However, non-permafrost peatlands are more productive and have higher C inputs than permafrost peatlands (Robinson and Moore, 2000; Jorgenson et al., 2001; Myers-Smith et al., 2008; O'Donnell et al., 2012), suggesting that even though large amounts of C may be lost through permafrost degradation, rapid C accumulation in collapse scar fens and non-permafrost peatlands may ultimately be greater than C loss over a long timescale.

5.4. Neoglacial Climate Cooling and Permafrost Aggradation in the Late Holocene

The onset of Neoglaciation following the HTM, which is ultimately due to decreasing summer insolation (Figure 10F), resulted in permafrost aggradation and glacier advances on the Seward Peninsula (Barclay et al., 2009; Jones et al., 2012), and increased sea-ice in the Bering Sea (Crockford and Frederick, 2007). The timing of Neoglaciation is highly variable across the Arctic, with the timing of cooling likely controlled by regional boundary conditions. In Alaska, many studies presented evidence for Neoglacial cooling beginning around 4.5 ka (e.g., Ellis and Calkin, 1984; Calkin et al., 1998; Levy et al., 2004; Crockford and Frederick, 2007). Both cores from this study indicate major changes occurring in the past 4.5 ka (Figure 10). In core NL10-1, C accumulation rates decrease and woody material dominates the site, while in core NL10-2 flood events disappear from the record and *Picea* and *Alnus* become major constituents on the landscape. In core NL10-1, the decrease in C accumulation rates to an average of 3.6 g C m^{-2} yr^{-1} at 4.5 ka is likely due to the aggradation of permafrost caused by Neoglacial cooling and drying of the soil (as a result of large uncertainty in the timing for this core in the past 4.5 ka, permafrost may have formed anytime between 4.5 and 2.5 ka). Oscillations in OM at site NL10-2 between 3.7 and 3 ka coincide with the reappearance of mineral material at site NL10-1 (Figures 10A and 10C). It is possible that there were periods of both permafrost aggradation and degradation between 3.7 and 3 ka at these sites, and that stable permafrost did not form until 2.5 ka. The significant increase in woody material after 4.5 ka also suggests drying and likely permafrost formation at site NL10-1 (Figure 10C).

At site NL10-2, average C accumulation rates were lower (14 g C m^{-2} yr^{-1}) at 4.5-0.8 ka than the long-term average of this peatland (21 g C m^{-2} yr^{-1}), also suggesting possible effect of Neoglacial climate cooling. This observation is in agreement with literature that suggests that C accumulation rates were high in the early Holocene and then declined after permafrost formation, with low rates especially over the past 4000 years in western Canada (Bauer and Vitt, 2011). Increased Cyperaceae in the pollen record and dominance by sedge in the macrofossil record (Figures 10E and 10D) suggests a wet climate initially. Multiple records indicate the migration of *Picea glauca* into southwestern Alaska at about 5.5 ka (Wright and Porter, 1984; Ager, 2003; Axford and Kaufman, 2004); however, *Picea* did not reach modern abundances in this record until about 2.5 ka, possibly due to soil moisture conditions (mesic conditions) favoring *Picea mariana* instead of *Picea glauca*, which migrated into the area later. Low *Picea* influx before 1 ka also suggests that *Picea mariana* likely migrated into this region before 1 ka and that *Picea glauca* did not become a major constituent in this region until after 1 ka. Increasing woody material after 2.5 ka in core NL10-2 (Figure 10D) and more Poaceae in the pollen record (Figure 10E) suggests a transition to dryer conditions.

More recently, the 20th century warming has reversed the long-term cooling trend of Neoglaciation (Hansen et al., 2006; Osterkamp et al., 2009; Kaufman et al., 2009; Chapin et al., 2010). In Alaska, a study from the Seward Peninsula indicates that thermokarst ponds have drained and shrunk in the past 50-100 years due to increased permafrost thaw (Yoshikawa and Hinzman, 2003). As permafrost thaws underneath a pond, an open talik forms and the surface water forms a direct connection to a sub- or intra-permafrost aquifer, causing pond water to drain. This leads to a drying pond surface and subsequent colonization by vegetation (Yoshikawa and HInzman, 2003). At this study site, similar changes can be seen between the aerial photos dated back to 1950, 1980, and 2009 (Figure 2). An overall drying trend on the landscape can be seen from these historical photos: what were thermokarst lakes in 1950 are now peatlands, likely due to the same phenomena discussed by Yoshikawa and Hinzman (2003). Major changes in vegetation and C accumulation can be seen in core NL10-2 over the past 100 years, but it is unclear whether warming/drier conditions or autogenic succession processes are responsible for the changes from rich fen to poor fen and enhanced C accumulation. Alternatively, at permafrost site NL10-1, there are no changes in C accumulation rates or vegetation in the past 100 years, perhaps because the permafrost underlying this site is stable. These results suggest that permafrost dynamics are highly dependant on local and small-scale factors, as the two study sites are only 30 m apart but experienced very different permafrost histories over the last several millennia. On the other hand, permafrost dynamics are also highly sensitive to climate change, as a slight increase in temperature can cause thawing, resulting in dramatic collapse of permafrost and subsequent drying.

6. Conclusions and Implication

1. The multiple proxy record from two cores shows the dynamic nature of the landscape and environment over the last 13,500 years. A warm climate during the BA and HTM was indicated by the presence of *Populus* in upland forests during the BA and HTM, and *Picea* during the BA. The anomalously high C accumulation rates from 13.5 to 12.7 ka are likely due to high plant productivity under a warmer climate during the BA, which may have led to permafrost thaw and collapse scar fen formation. Additionally, a more continental climate due to a lower sea level at that time may have limited cooling effects of sea ice in the Bering Sea. We speculate that the hiatus in the record at 12.8 to 9.1 ka was either due to dry climate during the Younger Dryas, or a catastrophic drainage or flooding event caused by rapid permafrost thaw or by river overbank flow that swept away sediments.

2. During the Holocene, a high OM content and dominance of *Sphagnum* characterize the very brief HTM period at 9.1-8.5 ka. Afterwards there are two main periods with distinct features: a warm/wet period with multiple flood events before 4.5 ka, and a relatively stable cool/dry period since 4.5 ka. Between 8 ka and 4.5 ka, the multiple oscillations between high OM and mineral-rich intervals (including sand-size grains) suggest possible recurrence of flooding events from the nearby Niukluk River or its tributaries at 8 ka, 6 ka, 5.4 ka, and 4.7 ka. However, a warm interval at 7-6 ka as indicated by a peak of *Alnus* and high OM separates the two early flooding events.

3. After 4.5 ka, a gradual increase in OM, the absence of flooding disturbances, and increase in trees and large shrubs (*Picea* and *Alnus*) suggest the stabilization of the local environment at the non-permafrost site. Permafrost aggradation at some locations, including at our permafrost site, in response to Neoglacial cooling and drying climate started at about 4.5 ka. We do not have any evidence for the presence of permafrost from two study sites in the study region before 4.5 ka likely because of a mild and very wet climate, but this needs to be confirmed by further studies.

4. The study site and likely the southern Seward Peninsula in general have experienced greater hydroclimate fluctuations and instability during the transition period at 8-4.5 ka, between the Holocene thermal maximum at 11 to 8.5 ka and Neoglaciation after 4.5 ka. Gradual declining summer insolation as a result of changes in orbital parameters is ultimately responsible for this climate transition, but sea-ice dynamics in nearby Bering Sea and Norton Sound might have provided important feedback to this environmental and ecological instability.

5. The abrupt increase in *Sphagnum* over the last 100 years may indicate thermokarst peatland response to recent warming, as a similar *Sphagnum* increase is observed during the HTM at the site. Alternatively, this may be the recent dramatic stage of continued succession of this peatland at the edge of a thermokarst lake, probably triggered and mediated by recent climate warming. Furthermore, aerial photographs indicate that 20th century warming has caused permafrost thaw that resulted in talik formation and subsequent colonization by vegetation, indicating that small increases in temperature can cause rapid ecosystem shifts even in ecosystems controlled largely by internal factors.

6. This study shows that regional climate has been a major control of permafrost and peatland dynamics, directly or indirectly through climate-induced disturbances. Moisture conditions appear to be an important feature of climate change that affect peatland and permafrost dynamics through their influence in part on flooding regimes.

Table 1: Lithology description of core NL10-2 based on observations in the field and of core photos.

Depth (cm)	Lithology
0-6	living and green *Sphagnum*
6-40	sedge peat
40-50	gap in peat core
100-117	well-preserved, dark peat
117-126	silty peat
126-137	humified organics with some silt
137-144	more silt rich with humified organics
144-165	organic rich, some silt
165-170	gray silt
170-173	well preserved peat
173-180	silt rich, organic peat
180-190	well-preserved peat
190-223	organics rich, some silt, with a sharp contact at 190 cm
223-247	gray silt
247-250	well-preserved peat
250-259	silt rich with peat laminations
259-274	organic rich, some silt
274-300	gray sand and coarse quartz sand

Table 2: Lithology description of permafrost core NL10-1 based on observations in the field and of core photos.

Depth (cm)	Lithology
0-63	well-preserved, un-frozen sedge peat
63-93	well-preserved peat
93-97	ice lens
98-119	ice-rich peat
119-123	well-preserved peat
123-125	ice-rich peat with some silt
125-163	ice-rich, sandy peat
163-178	ice-rich peat with some silt
178-198	less ice, well-preserved peat with some silt
198-256	ice and organic rich peat with some silt
256-274	organic rich peat with ice laminations
274-285	silt-rich peat with shells and wood
286-293	sand with shells

Table 3: Radiocarbon dates from cores NL10-1 and NL10-2 at the Niukluk Lake peatland, southern Seward Peninsula, Alaska.

UCIAMS Number *	Core	Depth (cm)	Material Dated	Sample Weight (mg)	^{14}C Date (yr BP)	Calibrated Age*** (cal yr BP) (2σ range)
97981	NL10-2	19	*Sphagnum* stems	3.2	115 ± 15	100 (42)
94505	NL10-2	35-37	*Chamaedaphne* leaf, *sphagnum* stems, wood fragments	3.7	1665 ± 20	1566 (45)
97982	NL10-2	62	Brown moss stems	2.3	4475 ± 45**	5135 (166)
88666	NL10-2	74	Wood fragment + *Carex* seed	4.1	3315 ± 15	3515 (68)
88667	NL10-2	95	*Sphagnum* stems + wood fragment	4.2	3995 ± 15	4492 (26)
97983	NL10-2	123	*Sphagnum* stems	2.2	4830 ± 70	5582 (135)
89819	NL10-2	137	*Sphagnum stems + wood fragment*	2.7	5680 ± 20	6451 (42)
94503	NL10-2	160	*Chamaedaphne* leaf, *sphagnum* stems, *carex* seeds, wood fragment	3	9125 ± 40 **	10313 (92)
94504	NL10-2	172	*Chamaedaphne* leaf, sphagnum stems, wood fragment	4.5	8295 ± 30**	9332 (96)
85702	NL10-2	188	*Sphagnum* stems	1.9	8190 ± 25	9090 (62)
88668	NL10-2	193	Carex seed + wood fragment	5	10965 ± 25	12809 (147)
85703	NL10-2	221	*Carex* seed + wood fragment + *Vaccinium* seed	3	10895 ± 25	12772 (131)
94506	NL10-2	252	*Carex* seed + *sphagnum* stems	2.5	11120 ± 35	12980 (149)
85704	NL10-2	258	*Carex* seed + wood fragment	2.9	11690 ± 35	13545 (148)
105034	NL10-1	7.5-10	Wood fragment	14.5	2390 ± 20	2407.5 (60.5)
105035	NL10-1	26-28.5	Wood fragment	9.4	4160 ± 20	4690.5 (75.5)
97984	NL10-1	46-48.5	Wood fragment	7.6	3545 ± 15	3857 (33)
97985	NL10-1	90-98	*Sphagnum* stems	6.6	4715 ± 15	5354.5 (27.5)
97986	NL10-1	140-148	Wood fragment	1097.5	5460 ± 15	6283.5 (13.5)
97987	NL10-1	208-220	Wood fragment	241.7	5630 ± 15	6422.5 (29.5)

Table 4: Results of grain size analysis at selected depths from core NL10-2 at the Niukluk Lake peatland complex on the Seward Peninsula, Alaska. Shown are percentage by weight for each size fraction. The percentage of grains larger than 125 μm is also summed and shown in the bottom row.

Depth (cm) **Age (Cal yr BP)**	**100** **4,662**	**120** **5,420**	**130** **5,995**	**170** **8,193**	**202** **12,981**
Size Fraction (μm)	**Percentage by weight**				
>500	2.1	3.5	2.3	1.1	1.7
250-500	21.2	13.7	26.3	11.4	17.5
150-250	28.0	7.4	32.0	27.3	22.6
125-150	7.0	5.6	6.8	6.2	6.4
63-125	28.4	34.8	21.1	36.6	36.6
<63	13.3	35.0	11.6	17.4	15.2
Total >125 μm fraction	51.3	24.6	60.6	39.7	41.8

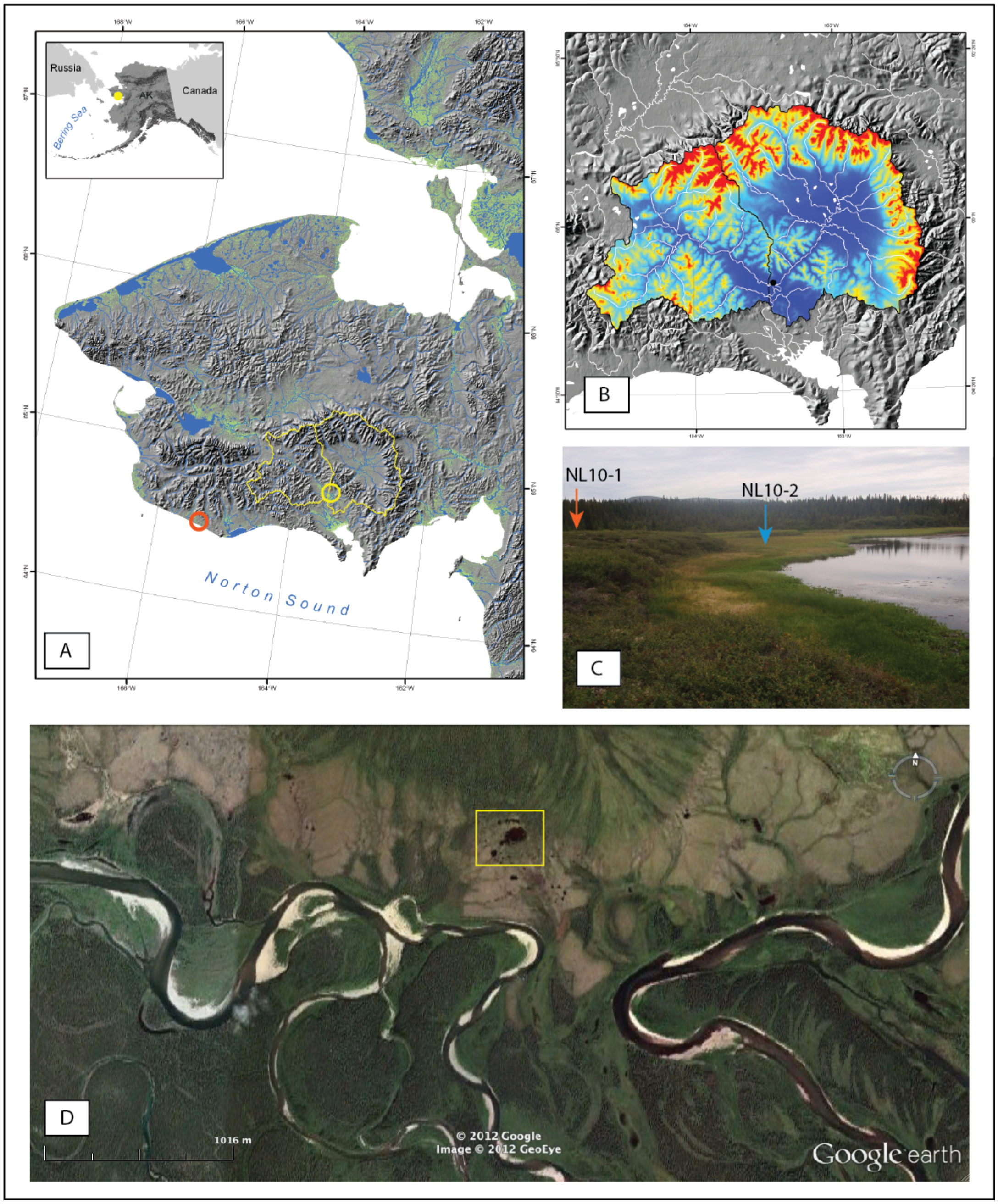

Figure 1: Maps and site information. **A.** Map of the Seward Peninsula showing the location of the study site near Niukluk Lake (yellow circle), the drainage basins (yellow outline) of the Niukluk (left) and Fish Rivers (right), and the location of Nome, Alaska (red circle). Wetland area is shown in green, and water bodies are shown in blue. The inset shows the location of the Seward Peninsula in Alaska. **B**. Digital Elevation Model showing the Niukluk Lake site in relation to the two drainage basins that may affect the site hydrologically. **C**.Photo of the coring sites near Niukluk Lake (open water to the right): permafrost core NL10-1 on the left (red arrow), and non-permafrost core NL10-2 on the edge of the thermokarst lake (blue arrow). **D**. Google Earth image taken in August 2009 showing the location of the study sites (yellow square) with respect to the Niukluk River (smaller river on left), which is a tributary of the Fish River (large river).

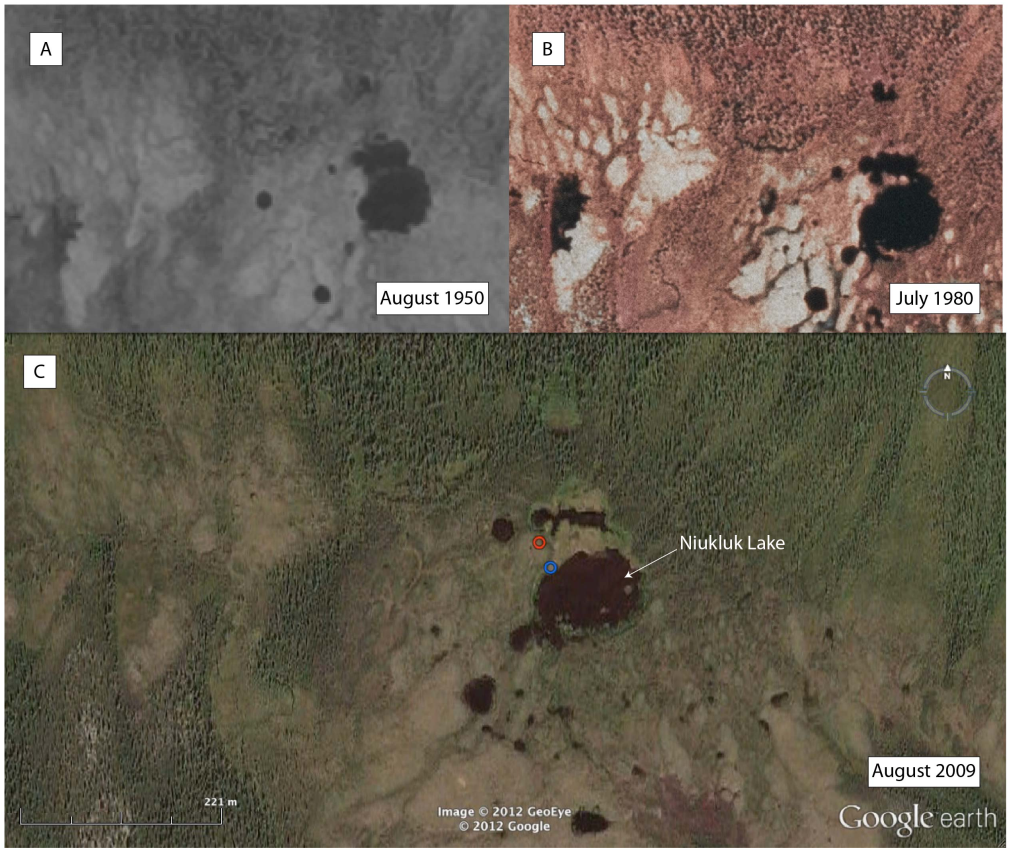

Figure 2: Historical aerial photographs of the Niukluk Lake area. **A.** Aerial photograph from August, 1950. (Source: USGS). **B.** Infrared aerial photograph from July, 1980, showing the study site (Source: USGS). **C.** Google Earth image from August, 2009, showing the study site (Source: Google Earth). Coring locations shown with the blue circle (NL10-2) and red circle (NL10-1).

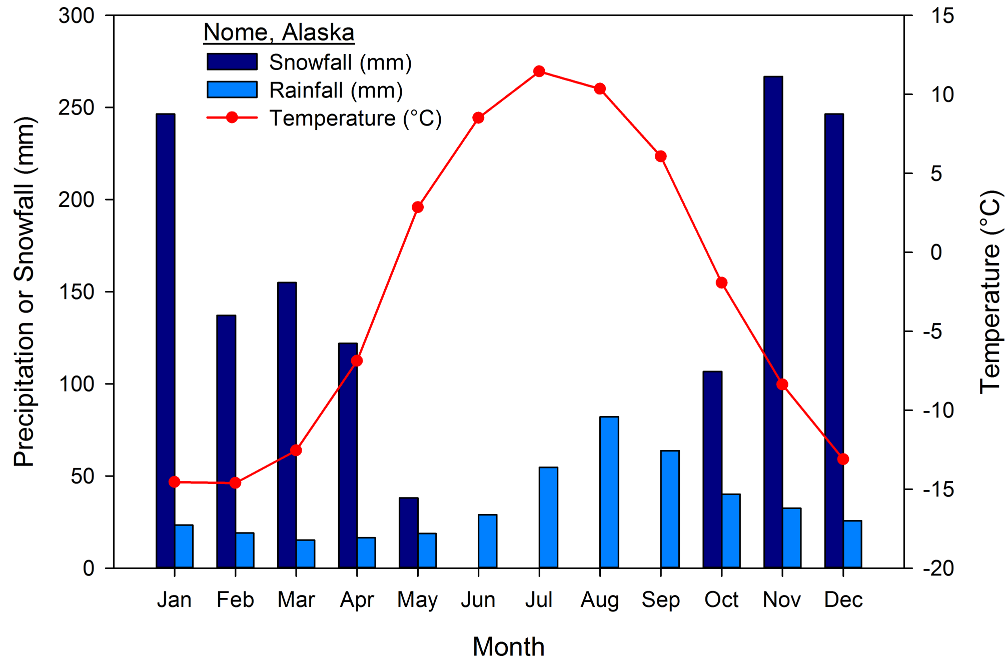

Figure 3: Climate data for Nome, Alaska. Monthly means are based on the period 1971-2000. Snowfall averages are the dark blue bars (in mm), precipitation averages are the light blue bars (in mm), and temperatures averages are the red symbols (in °C). Data from NOAA.

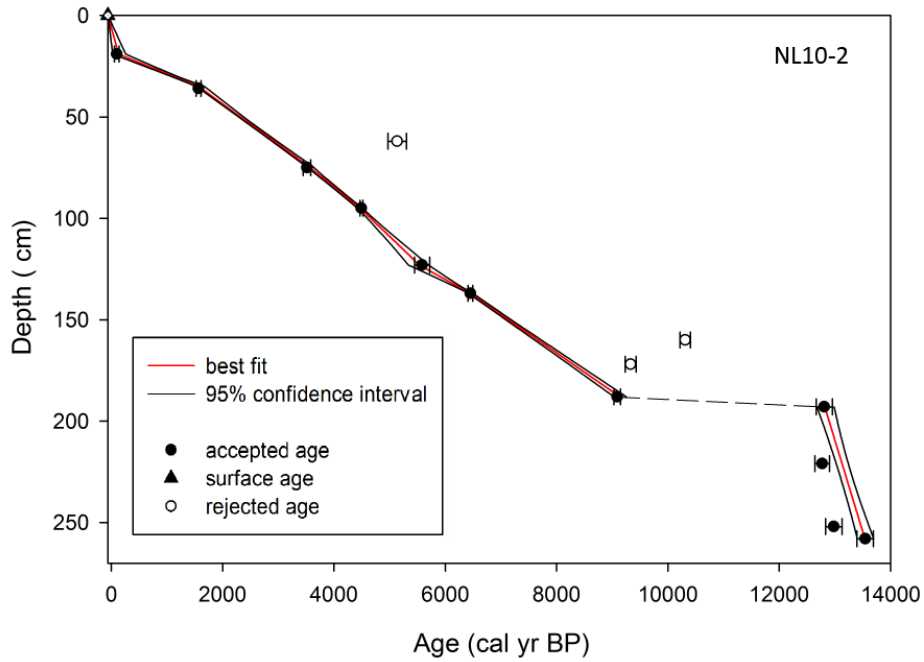

Figure 4: Age-depth model for core NL10-2 at the Niukluk Lake peatland complex. Age-model is based on linear interpolation between accepted calibrated ages (n=11) using program Clam for two intervals before and after the hiatus (dashed line). Open circles indicate ages not included in age models. The triangle is the surface age.

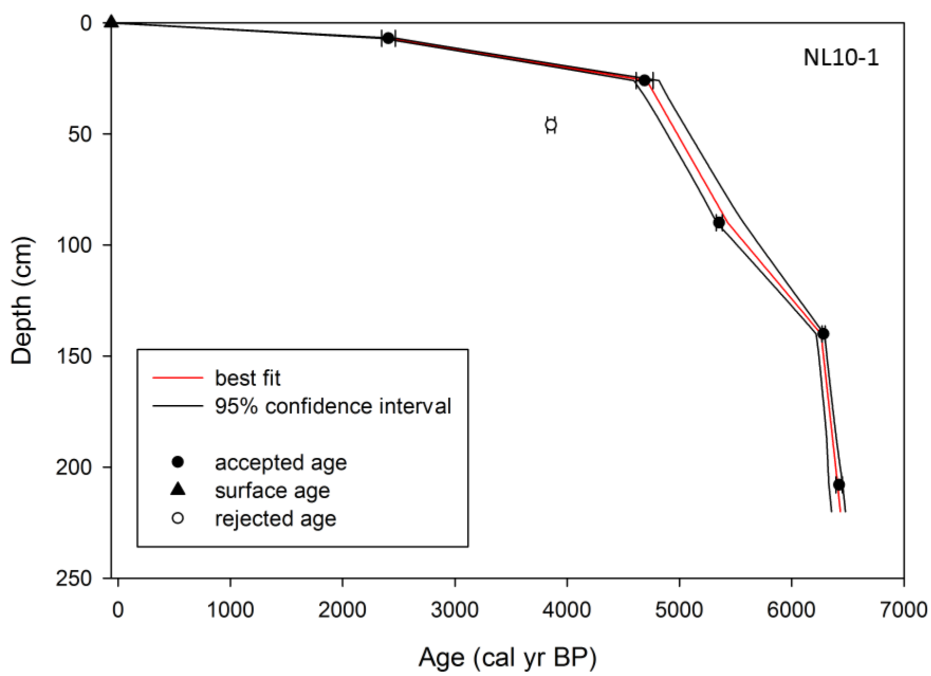

Figure 5: Age-depth model for core NL10-1 at the Niukluk Lake peatland complex. Age-depth model is based on linear interpolation between calibrated ages (n=5). Open circle indicates age not included in age model. The triangle is the surface age.

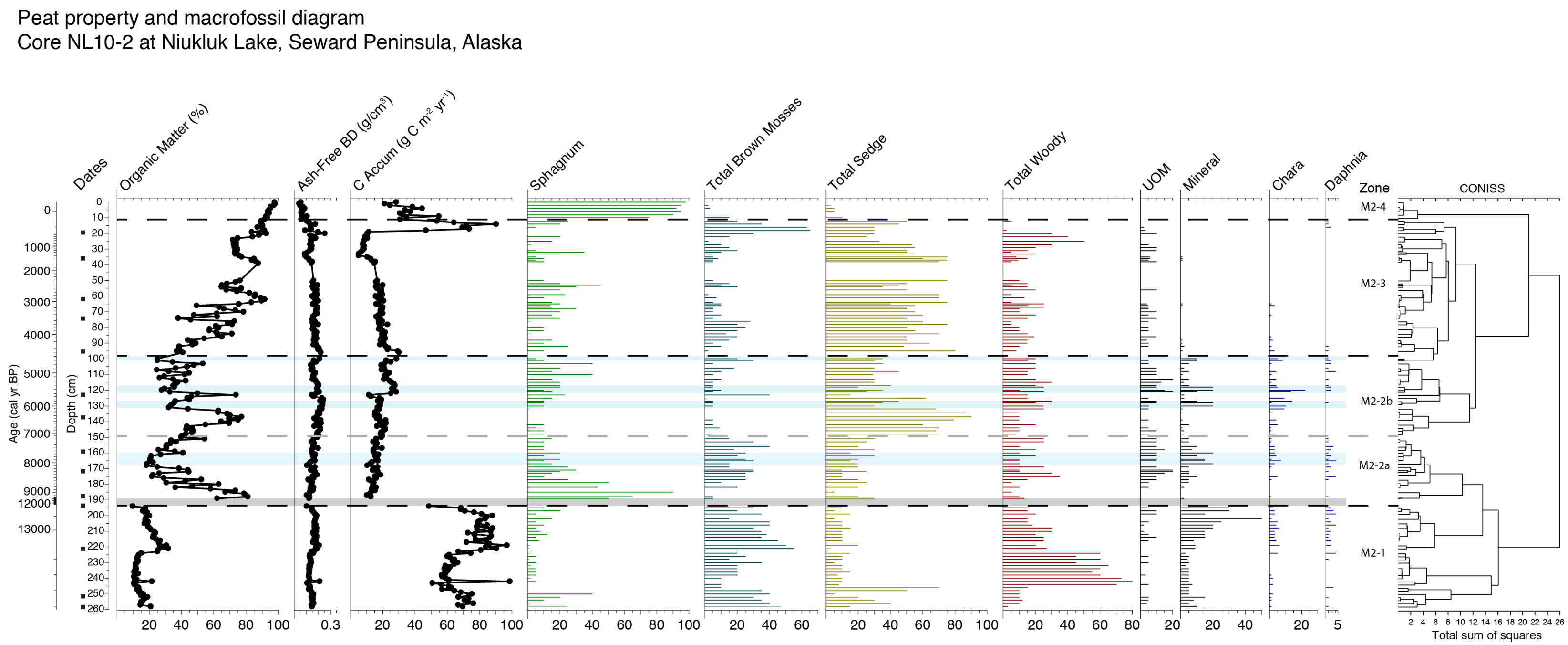

Figure 6: Summary macrofossil and LOI results from non-permafrost core NL10-2 at the Niukluk Lake peatland complex. Depths of dating samples are shown with black squares to the left of the primary depth axis. All are shown as percent of total sample by volume except for ash-free bulk density (g/cm^3), C accumulation rates (g C m^{-2} yr^{-1}), and *Chara* oospore and *Daphnia* epilobium (counts). Flood events are displayed by light-blue shading. Zones are shown with a black dashed line and subzones are shown with a grey dashed line, and were identified with the aid of CONISS cluster analysis (shown on the right). Mineral material is greater than 125 µm.

Peat property and macrofossil diagram
Core NL10-1 at Niukluk Lake, Seward Peninsula, Alaska

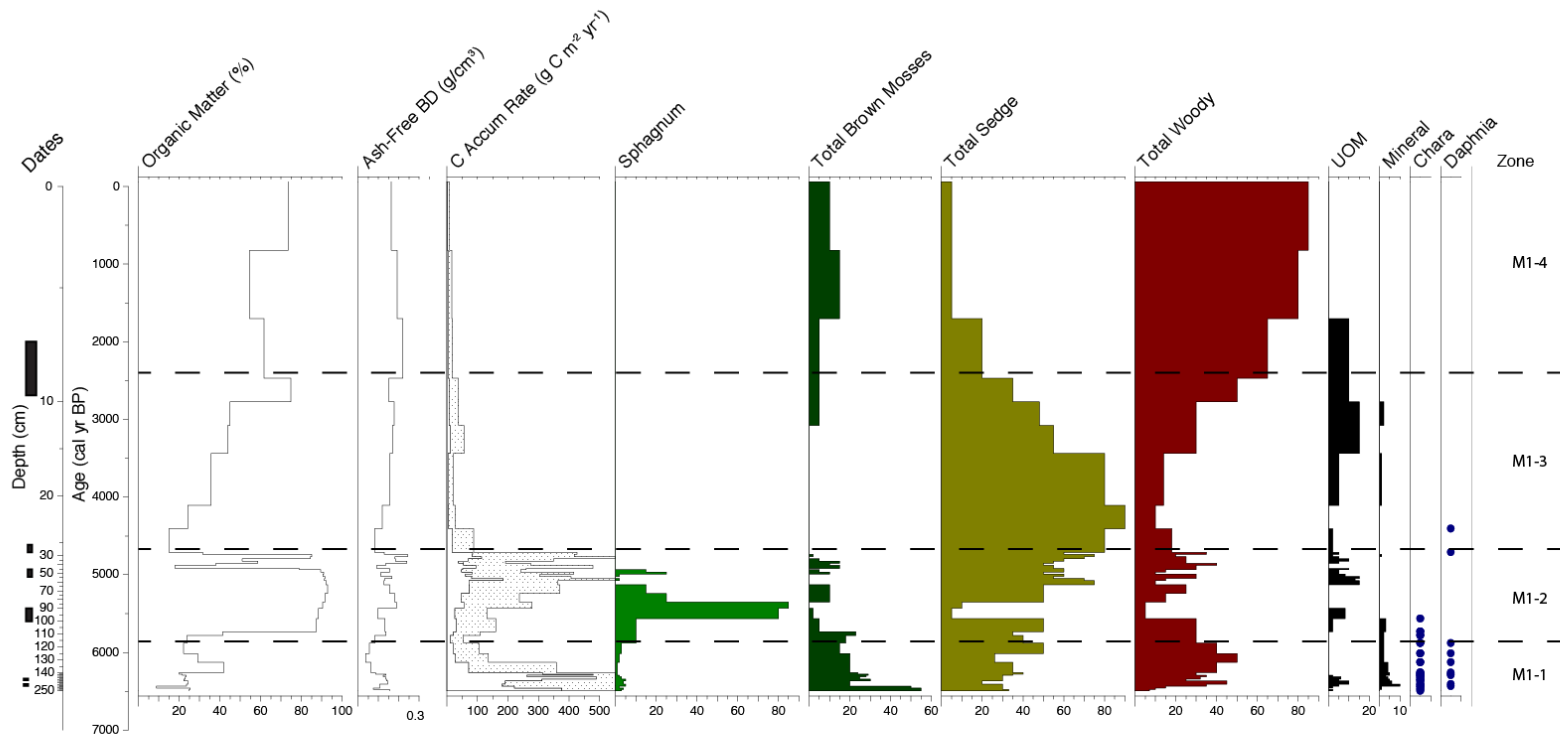

Figure 7: Summary macrofossil and LOI results from permafrost core NL10-1 at the Niukluk Lake peatland complex. Depths of dating samples are shown with black squares to the left of the depth axis. All are shown as percent of total sample by volume except for ash-free bulk density (g/cm^3), C accumulation rates (g C m^{-2} yr^{-1}), and *Chara* oospore and *Daphnia* epilobium (presence or absence). Zones are shown with a black dashed line and labeled to the right of the figure.

Pollen diagram of core NL10-2, Niukluk Lake peatland, Alaska

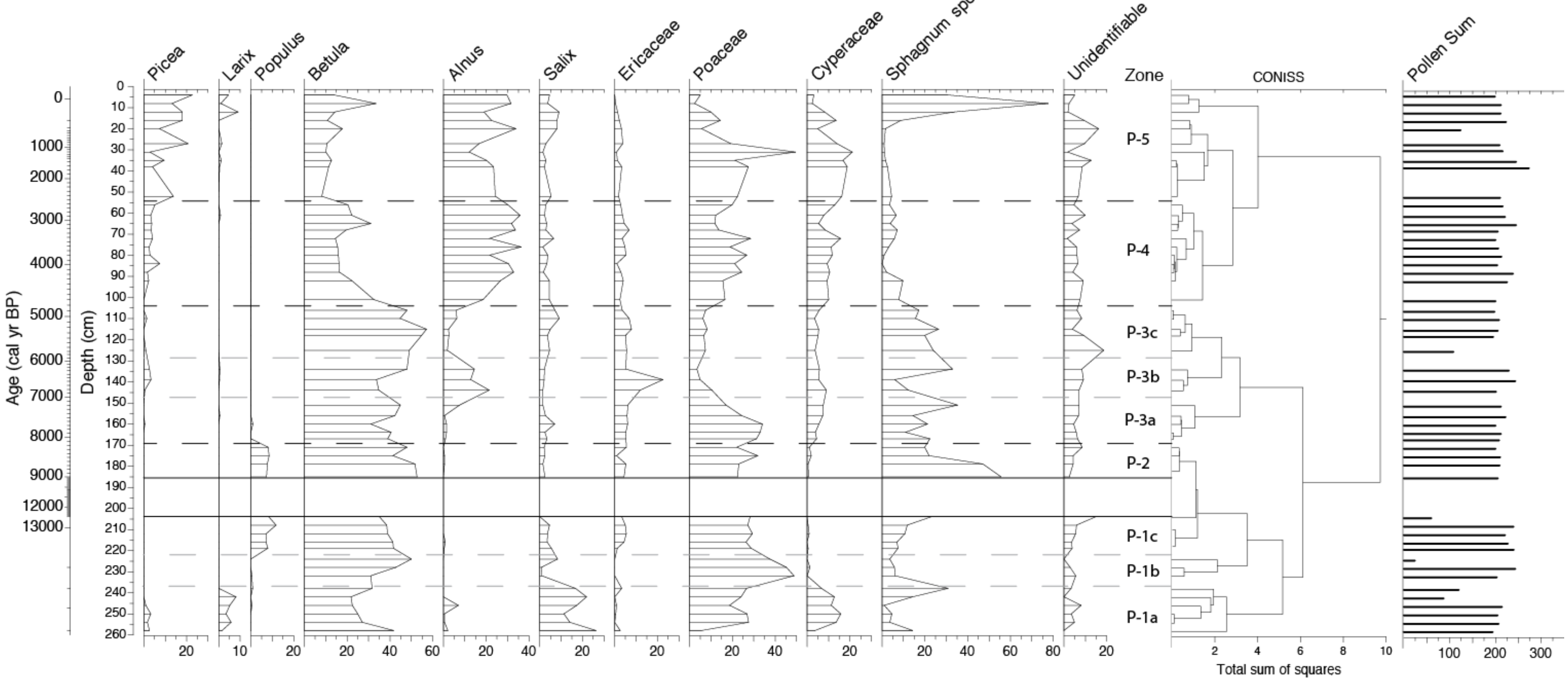

Figure 8: Pollen percentage diagram for core NL10-2 at the Niukluk Lake peatland complex. *Sphagnum* spores are shown as percent of total upland pollen grains and spores. Zones are shown with a black dashed line and subzones are shown with a grey dashed line, and were identified with the aid of CONISS cluster analysis. Pollen count for each sample is on the right of the diagram.

Pollen concentration, pollen influx, and *Picea* influx
Core NL10-2, Niukluk Lake, Seward Peninsula, AK

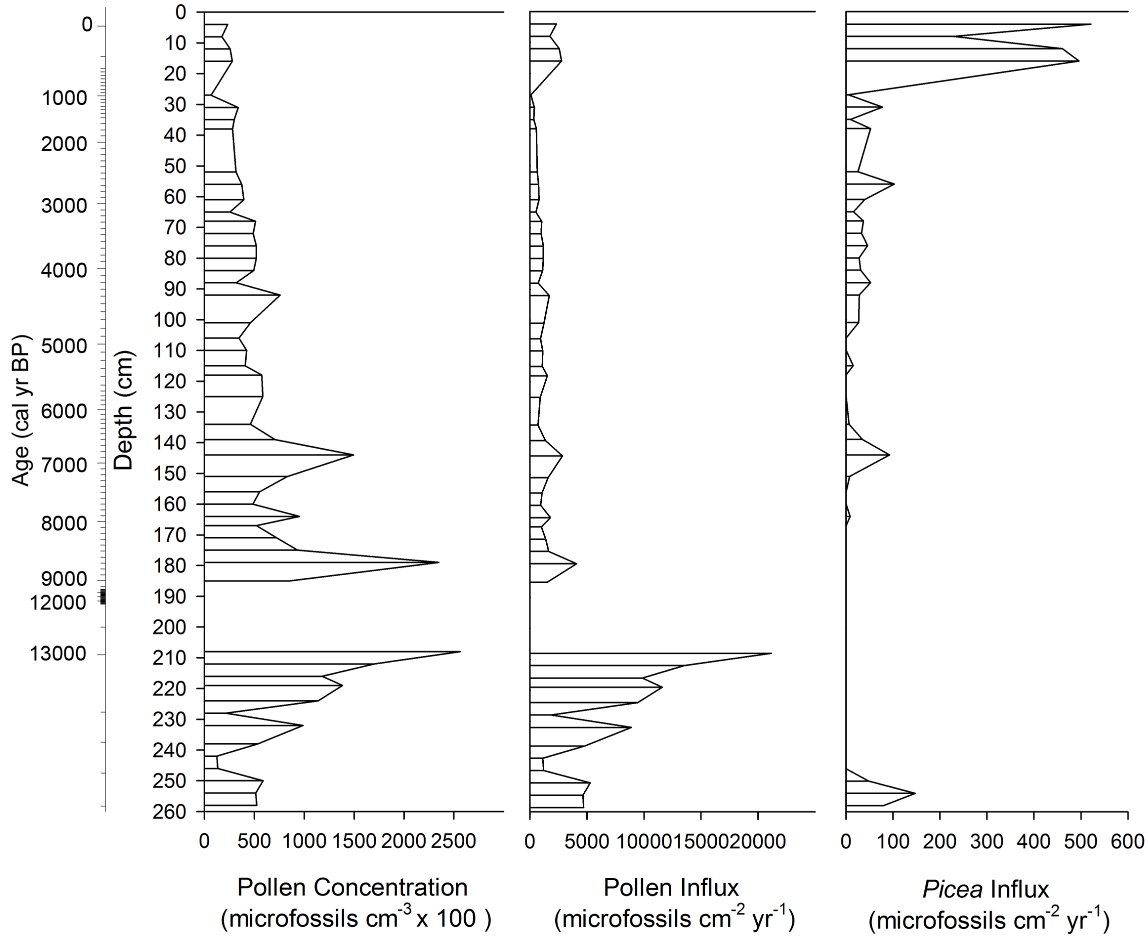

Figure 9: Pollen influx and concentration diagram for core NL10-2 at the Niukluk Lake Peatland complex. Pollen concentration is shown as microfossils cm^{-3} x 100, pollen influx is shown as microfossils cm^{-2} yr^{-1}, and *Picea* influx is shown as microfossils of *Picea* cm^{-2} yr^{-1}.

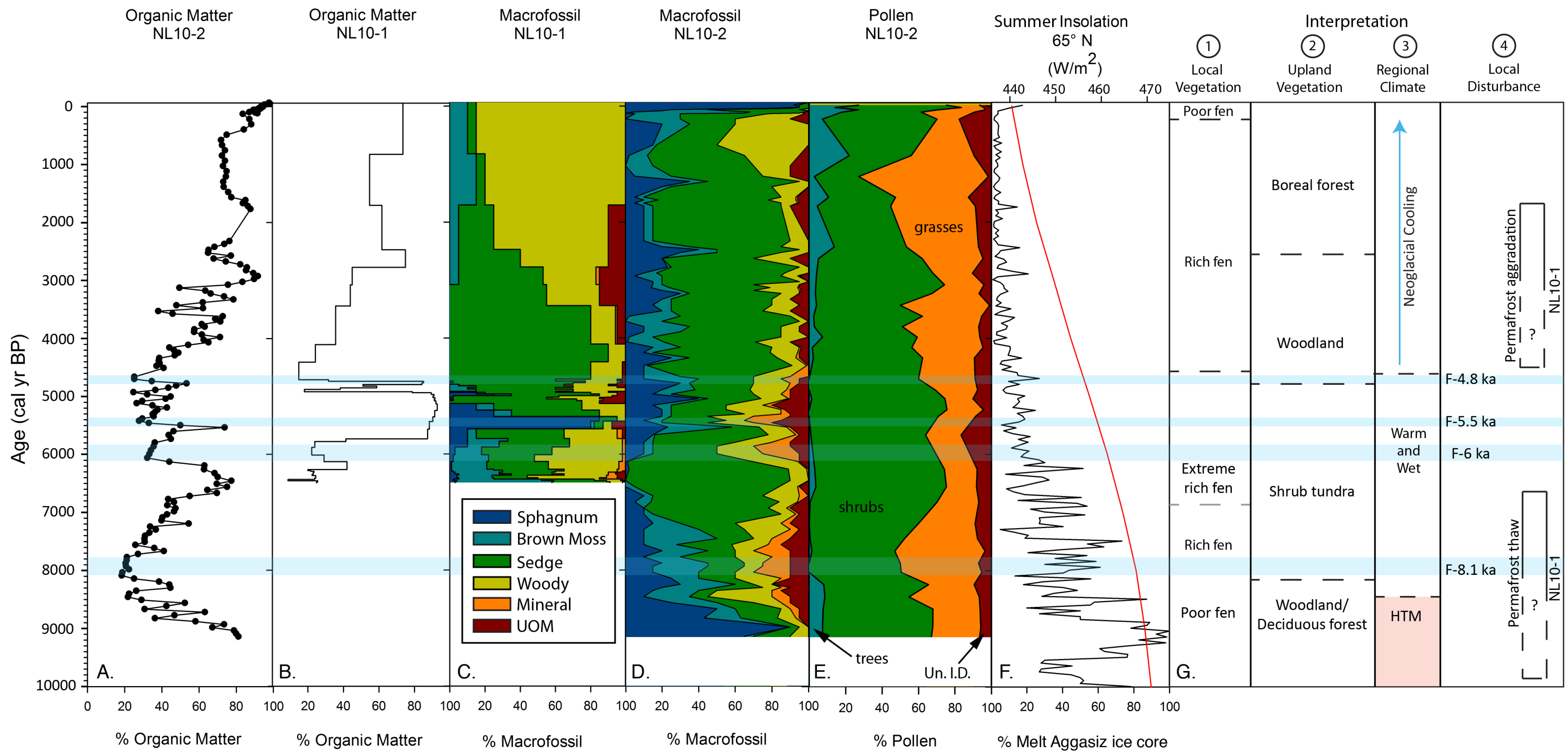

Figure 10: Correlation diagram for the past 10,000 years. Panels A and B display the OM content (%) for cores NL10-2 and core NL10-1, respectively. Panels C and D display the results of macrofossil analysis for cores NL10-1 and NL10-2, respectively. The key refers to both macrofossil records. UOM indicates unidentifiable organic matter. Panel E shows the summary diagram of pollen results from core NL10-2. Pollen types were placed into groups: Trees (blue), shrubs (green), grasses (orange), and unidentified (red). Panel F displays summer insolation at 65 °N (adapted from Huybers, 2006) and % melt of the Agassiz Ice Cap in northern Canada (from Fisher et al., 1994 and Fisher et al., 1995). Panel G(1-4) displays the interpretations of the various records. G1 shows the local vegetation interpretation, and macrofossil zones are indicted with a dashed line, G2 shows the upland/regional vegetation interpretation, and pollen zones are indicated with dashed lines. G3 shows the general climatic conditions, and G4 shows the interpretations on disturbance. Flood events are shown with light blue shading.

LIST OF REFERENCES

Abbott, M.B., Edwards, M.E., Finney, B.P., 2010. A 40,000-year record of environmental change from Burial Lake in northwest Alaska. Quaternary Research 74, 156–165.

Ager, T., 2003. Late Quaternary vegetation and climate history of the central Bering land bridge from St. Michael Island, western Alaska. Quaternary Research 60, 19-32.

Anderson, P.M., Brubaker, L.B., 1994. Vegetation history of north central Alaska: a mapped summary of late-Quaternary pollen data. Quaternary Science Reviews 13, 71–92.

Axford, Y., 2000. Late Quaternary glacier fluctuations and vegetation change in the northwestern Ahklun Mountains, southwestern Alaska. M.Sc. thesis. Logan, Utah: Utah State University. 193 pp.

Axford, Y. and Kaufman, D., 2004. Late Glacial and Holocene Glacier and Vegetation Fluctuations at Little Swift Lake, Southwestern Alaska. Arctic, Antarctic, and Alpine Research 36, 139-146.

Barclay, D., Wiles, G., Calkin, P., 2009. Holocene glacier fluctuations in Alaska. Quaternary Science Reviews 28, 2034-2048.

Bauer, I., Vitt, D., 2011. Peatland dynamics in a complex landscape: Development of a fen-bog complex in the Sporadic Discontinuous Permafrost zone of northern Alberta, Canada. Boreas 40, 714-726.

Beilman, D.W., MacDonald, G.M., Yu, Z., 2010. The northern peatland carbon pool and the Holocene carbon cycle. PAGES News 18, 22-24.

Berger, A., and M.F. Loutre., 1991. Insolation values for the climate of the last 10 million of years. Quaternary Science Reviews 10, 297-317.

Bhiry, N., Payette, S., Robert, E., 2007. Peatland development at the arctic tree line (Quebec, Canada) influenced by flooding and permafrost. Quaternary Research 67, 426-437.

Blaauw, M., 2010. Methods and code for 'classical' age-modeling of radiocarbon sequences. Quaternary Geochronology 5, 512-518.

Brosius, L., Walter-Anthony, K., Grosse, G., Chanton, J., Farquharson, L., Overduin, P., Meyer, H., 2012. Using the deuterium isotope composition of permafrost meltwater to constrain thermokarst lake contributions to atmospheric CH_4 during the last deglaciation. Journal of Geophysical Research 117, G01022, 16 pp.

Brown J., Ferrians O.J Jr, Heginbottom J.A, Melnikov E.S., 1998. Circum-Arctic Map of Permafrost and Ground-Ice Conditions. Boulder (CO): National Snow and Ice Data Center/World Data Center for Glaciology.

CAFF. 2001. Arctic flora and fauna status and conservation. Arctic Council.

Camill, P., Lynch, J., Clark, J., Adams, J., Jordan, B., 2001. Changes in Biomass, Aboveground Net Primary Production, and Peat Accumulation Following Permafrost Thaw in the Boreal Peatlands of Manitoba, Canada. Ecosystems 4, 461-478.

Calkin, P., Kaufman, D., Przybyl, B., Whitford, W., Peck, B., 1998, Glacier regimes, periglacial landforms, and Holocene climate change in the Kigluaik Mountains, Seward Peninsula, Alaska, U.S.A.: Arctic and Alpine Research 20, 154-165.

Calmels, F., Gagnon, O., Allard, M., 2005. A portable earth-drill system for permafrost studies. Permafrost and Periglacial Processes 16, 311-315.

Carter, L.D., 1993. Late Pleistocene stabilization and reactivation of eolian sand in northern Alaska: implications for the effects of future climatic warming on an eolian landscape in continuous permafrost. In Proceedings of the Sixth International Conference on Permafrost. South China University of Technology Press: Wushan Guangzhou, China; 78–83.

Chapin, F., McGuire, A., Ruess, R., Hollingsworth, T., Mack, M., Johnstone, J., Kasischke, E., Euskirchen, E., Jones, J., Jorgenson, M., Kielland, K., Kofinas, G., Turetsky, M., Yarie, J., Lloyd, A., Taylor, D., 2010. Resilience of Alaska's boreal forest to climatic change. Canadian Journal of Forest Research 40, 1360-1370.

Churchill, A., 2011. The response of plant community structure and productivity to changes in hydrology in Alaskan boreal peatlands. Masters Thesis, University of Alaska Fairbanks.

Côte, M., Burn, S., 2002. The oriented lakes of Tuktoyaktuk Peninsula, Western Arctic Coast, Canada: a GIS-based analysis, Permafrost and Periglacial Processes 13, 61-70.

Crockford, S., Frederick, S., 2007. Sea ice expansion in the Bering Sea during the Neoglacial: evidence from archaeozoology. The Holocene 17, 699-706.

Cwynar L.C., Spear R.W., 1995. Paleovegetation and paleoclimatic changes in the Yukon at 6 ka yr B. P. Geogr Phys Quat 49, 29-35.

Davies, M., Mix, A., Stoner, J., Addison, J., Jaeger, J., Finney, B., Wiest, J., 2011. The deglacial transition on the southeastern Alaska Margin: Meltwater input, sea level rise, marine productivity, and sedimentary anoxia. Paleoceanography 26, PA 2223, 18 pp.

Donnelly et al., 2004. Catastrophic meltwater discharge down the Hudson Valley: A potential trigger for the Intra-Allerod cold period. Geology 33, 89-92.

Edwards, M., Mock, C., Finney, B., Barber, V., Bartlein, P., 2001. Potential analogues for paleoclimatic variations in eastern interior Alaska during the past 14,000 yr: atmospheric-circulation controls of regional temperature and moisture responses. Quaternary Science Reviews 20, 189-202.

Edwards, M.E., Brubaker, L.B., Lozhkin, A.V., Anderson, P.M., 2005. Structurally novel biomes: a response to past warming in Beringia. Ecology 86, 1696-1703.

Ellis, J.M., Calkin, P.E., 1984. Chronology of Holocene glaciation, central Brooks Range, Alaska. Bulletin of the Geological Society of America 95, 897-912.

Fægri, K., Iversen, J., 1989: Textbook of pollen analysis (4th Edition). John Wiley and Sons, London, UK. 216 pp.

Fisher, D. A., Koerner, R. M., 1994. Signal and Noise in Four Ice-Core Records from the Agassiz Ice Cap, Ellesmere Island, Canada: Details of the Last Millennium for stable isotopes, melt and solid conductivity. The Holocene 4, 113-120.

Fisher, D. A., Koerner, R. M., Reeh, N., 1995. Holocene Climatic Records from Agassiz Ice Cap, Ellesmere Island, NWT, Canada. The Holocene 5, 19-24.

Gorham, E., 1991. Northern Peatlands: Role in the Carbon Cycle and Probable Responses to Climatic Warming. Ecological Applications 1, 182-195.

Grimm, E.C., 1987. CONISS: a FORTRAN 77 program for stratigraphically constrained cluster analysis by the method of incremental sum of squares. Computers and Geosciences 13, 13-55.

Grimm, E.C., 1992. Tilia and Tilia-graph: pollen spreadsheet and graphics programs. Program and Abstracts, 8th International Palynological Congress, Aix-en-Provence [France], September 6-12, 1992, 56 pp.

Hansen, J., Sato, M., Ruedy, R., Lo, K., Lea, D., Medina-Elizade, M., 2006. Global temperature change. Proceedings of the National Academy of Sciences of the United States of America 103, 14288-14293.

Hinkel, K.M., Jones, B.M., Eisner, W.R., Cuomo, C.J., Beck, R.A., Frohn, R., 2007. Methods to assess natural and anthropogenic thaw lake drainage on the western Arctic coastal plain of northern Alaska, Journal of Geophysical Research 112, F02S16, 9 pp.

Hinzman et al., 2005. Evidence and implications of recent climate change in Northern Alaska and other Arctic regions. Climate Change 72, 251-298.

Hu et al., 2001. Effects of Holocene *Alnus* Expansion on Aquatic Productivity, Nitrogen Cycling, and Soil Development in Southwestern Alaska. Ecosystems 4, 358-368.

Hu, F. S., Lee, B.Y., Kaufman, D.S., Yoneji, S., Nelson, D.M., Henne, P.D., 2002. Response of tundra ecosystem in southwestern Alaska to Younger-Dryas climatic oscillation. Global Change Biology 8, 1156–1163.

Hunt, S., 2010. Response of Peatland Carbon Accumulation to Late Holocene Climate Change in South-Central Alaska. Undergraduate Honors Thesis, Bethlehem, PA: Lehigh University. 35 pp.

IPCC (Intergovernmental Panel on Climate Change)., 2007. Climate change 2007: the physical science basis. Summary for policymakers. Geneva, Switzerland: Intergovernmental Panel on Climate Change.

Jones, M. C., Yu, Z., 2010. Rapid deglacial and early Holocene expansion of peatlands in Alaska, Proceedings of the National Academy of Sciences of the United States of America 107, 7347–7352.

Jones, M., Grosse, G., Jones, B., Anthony, K., 2012. Peat accumulation in drained thermokarst lake basins in continuous, ice-rich permafrost, northern Seward Peninsula, Alaska Journal of Geophysical Research 117, G00M07, 16 pp.

Jorgenson, M., Racine, C., Walters, J., Osterkamp, T., 2001. Permafrost Degradation and Ecological Changes Associated with a Warming Climate in Central Alaska. Climatic Change 48, 551-579.

Kaufman, D.S., Ager, T.A., Anderson, N.J., Anderson, P.M., Andrews, J.T., Bartlein, P.J., Brubaker, L.B., Coats, L.L., Cwynar, L.C., Duvall, M.L., Dyke, A.S., Edwards, M.E., Eisner, W.R., Gajewski, K., Geirsdottir, A., Hu, F.S., Jennings, A.E., Kaplan, M.R., Kerwin, M.W., Lozhkin, A.V., MacDonald, G.M., Miller, G.H., Mock, C.J., Oswald, W.W., Otto-Bliesner, B.L., Porinchu, D.F., Ruhland, K., Smol, J.P., Steig, E.J., Wolfe, B.B., 2004. Holocene thermal maximum in the western Arctic (0–180 degrees W). Quaternary Science Reviews 23, 529–560.

Kaufman, D., Scneider, D., McKay, N., Ammann, C., Bradley, R., Briffa, K., Miller, G., Otto-Bliesner, B., Overpeck, J., Vinther, B., Arctic Lakes 2k Project Members., 2009. Recent Warming Reverses Long-Term Arctic Cooling. Science 325, 1236-1239.

Kaufman et al., 2010. Evidence for a variable and wet Younger Dryas in Southern Alaska. Quaternary Science Reviews 29, 1445-1452.

Kelly C.A., Rudd, J.M., Bodaly, R.A., Roulet, N.T., St. Louis, V.L., Heyes, A., Moore, T.R., Schiff, S., Aravena, R., Scott, K.J., Dyck, B., Harris, R., Warner, B., Edwards, G., 1997. Increases in fluxes of greenhouse gases and methyl mercury following flooding of an experimental reservoir. Environ Sci Technol 31, 1334–1344.

Kokorowski, H., Anderson, P., Mock, C., Lozhkin, A., 2008. A re-evaluation and spatial analysis of evidence for a Younger Dryas climatic reversal in Beringia. Quaternary Science Reviews 27, 1710-1722.

Levy, L.B., Kaufman, D.S., Werner, A., 2004. Holocene glacier fluctuations, Waskey Lake, northeastern Ahklun Mountains, southwestern Alaska. The Holocene 14, 185–193.

Lozhkin, A., Anderson, P., Eisner, W., Solomatkina, T., 2011. Late glacial and Holocene landscapes of central Beringia. Quaternary Research 76, 383-392.

MacDonald, G., Beilman, D., Kremenetski, K., Sheng, Y., Smith, L., Velichko, A., 2006. Rapid Early Development of Circumarctic Peatlands and Atmospheric CH4 and CO2 Variations. Science 314, 285-288.

Mann, D., Peteet, D., Reanier, R., Kunz, M., 2002a. Responses of an arctic landscape to Lateglacial and early Holocene climatic changes: the importance of moisture. Quaternary Science Reviews 21, 997-1021.

Mann, D., Heiser, P., Finney, B., 2002b. Holocene history of the Great Kobuk Sand Dunes, Northwestern Alaska. Quaternary Science Reviews 21, 709-731.

Mann, D., Groves, P., Reanier, R., Kunz, M., 2010. Floodplains, permafrost, cottonwood trees, and peat: What happened the last time climate warmed suddenly in arctic Alaska? Quaternary Science Reviews 29, 3812-3830.

McGuire et al., 2009. Sensitivity of the Carbon Cycle in the Arctic to Climate Change. Ecological Monographs 79, 523-555.

Moritz, R., Bitz, C., Steig, E., 2002. Dynamics of Recent Climate Change in the Arctic. Science 297, 1497-1502.

Myers-Smith, I., Harden, J., Wilmking, M., Fuller, C., McGuire, A., Chapin III, F., 2008. Wetland succession in a permafrost collapse: Interactions between fire and thermokarst. Biogeosciences 5, 1273–1286.

NOAA, U.S. Climate Normals 1971-2000, www.ncdc.noaa.gov/normals.html

O'Donnell, J., Jorgenson, M., Harden, J., McGuire, D., Kanevskiy, M., Wickland, K., 2012. The Effects of Permafrost Thaw on Soil Hydrologic, Thermal, and Carbon Dynamics in an Alaska Peatland. Ecosystems 15, 213-229.

Osterkamp, T. E., Jorgenson, M. T., Schuur, E. A. G., Shur, Y. L., Kanevskiy, M. Z., Vogel, J., 2009. Physical and ecological changes associated with warming permafrost and thermokarst in interior Alaska. Permafrost and Periglacial Processes 20, 235-256.

Overpeck, J. et al., 1997. Arctic Environmental change of the last four centuries. Science 278, 1251-1256.

Peteet, D. M., Mann, D. H., 1994: Late-glacial vegetation, tephra, and climatic history of southwestern Kodiak Island, Alaska. Ecoscience 1, 255–267.

Peteet, D., Andreev, A., Bardeen, W., Mistretta, F., 1998. Long-term Arctic peatland dynamics, vegetation and climate history of the PurTaz region, western Siberia. Boreas 27, 115-126.

Reimer P.J., Baillie M.G.L., Bard E., Bayliss A., Beck J.W., Blackwell P.G., Bronk Ramsey C., Buck C.E., Burr G.S., Edwards R.L., Friedrich M., Grootes P.M., Guilderson T.P., Hajdas I., Heaton T.J., Hogg A.G., Hughen K.A., Kaiser K.F., Kromer B., McCormac F.G., Manning S.W., Reimer R.W., Richards D.A., Southon J.R., Talamo S., Turney C.S.M., van der Plicht J., Weyhenmeyer C.E., 2009. IntCal09 and Marine09 radiocarbon age calibration curves, 0–50,000 years cal BP. Radiocarbon 51, 1111–50.

Robinson, S., Moore, T., 2000. The influence of permafrost and fire upon carbon accumulation in high boreal peatlands, Northwest Territories, Canada. Arctic, Antarctic, and Alpine Research 32**,** 155-166.

Roulet N.T., Lafleurs, P.M., Richard, P.J.H., Moore, T.R., Humphreys, E.R., Bubier, J., 2007. Contemporary carbon balance and late Holocene carbon accumulation in a northern peatland. Global Change Biology 13**,** 397-411.

Turetsky, M., Wieder, R., Vitt, D., 2002. Boreal peatland C fluxes under varying permafrost regimes. Soil Biology and Biochemistry 34, 907-912.

Turunen et al., 2001. Carbon accumulation in West Siberian Mires, Russia. Global Biogeochemical Cycles 15, 285–296.

Schuur, E., Vogel, J., Crummer, K., Lee, H., Sickman, J., Osterkamp, T., 2009. The effect of permafrost thaw on old carbon release and net carbon exchange from tundra. Nature 459, 556-559.

Statewide Alaska Geology compiled by Greenhorne & O'Mara, Inc, 1999. Data compiled from 1955 and 1960 USGS maps.

St Louis, V., Kelly, C., Duchemin, E., Rudd, J., Rosenberg, D., 2000. Reservoir surfaces as sources of greenhouse gases to the atmosphere: a global estimate. BioScience 50, 766–775.

Stuiver, M., Reimer, P.J., 1993. Extended 14C data base and revised CALIB 3.0 14C age calibration program. Radiocarbon 35, 215-230.

Tarnocai, C., Canadell, J., Schuur, E., Kuhry, P., Mazhitova, G., Zimov, S., 2009. Soil organic carbon pools in the northern circumpolar permafrost region. Global Biogeochemical Cycles 23, GB2023, 11 pp.

Vitt, D., Halsey, L., Zoltai, S., 1994. The bog landforms of continental Western Canada in relation to climate and permafrost patterns. Arctic and Alpine Research 26, 1-13.

Walter, K.M., Edwards, M.E., Grosse, G., Zimov, S.A., Chapin III, F., 2007. Thermokarst lakes as a source of atmospheric CH4 during the last deglaciation. Science 318, 633–636.

Wassen, M.J.,Barendregt, A., Palczynksi, A., de Smidt, J.T., de Mars, H., 1990. The relationship between fen vegetation gradients, groundwater flow, and flooding in an undrained valley mire at Biebrza, Poland. Journal of Ecology 68, 1106-1122.

Wright, H., Porter, S., 1984. Late-Quaternary Environments of the United States: The late Pleistocene. Minneapolis (Minnesota): University of Minnesota Press. 433 pp.

Yershov, E.,1998. General Geocryology. Cambridge (United Kingdom): Cambridge University Press. 608 pp.

Yoshikawa, K., Hinzman, L., 2003. Shrinking Thermokarst Ponds and Groundwater Dynamics in Discontinuous Permafrost near Council, Alaska. Permafrost and Periglacial Processes 14, 151-160.

Yu, Z., Walker, K., Evenson, E., Hajdas, I., 2008. Lateglacial and early Holocene climate oscillations in the Matanuska Valley, south-central Alaska. Quaternary Science Reviews 27, 148-161.

Yu, Z., Beilman, D., Jones, M., 2009. Sensitivity of northern peatland carbon dynamics to Holocene climate change. Geophysical Monograph Series: Carbon cycling in northern peatlands 184, 55-70.

Yu, Z., Loisel, J., Brosseau, D., Beilman, D., Hunt, S., 2010. Global peatland dynamics since the Last Glacial Maximum. Geophysical Research Letters 37, L13402, 5 pp.

Zhang, T., Barry, R.G., Knowles, K., Heginbottom, J.A., Brown, J., 1999. Statistics and characteristics of permafrost and ground-ice distribution in the Northern Hemisphere. Polar Geography 23, 132–154.

Stephanie J Hunt

1238D Seidersville Rd, Bethlehem, Pennsylvania, 18015
(856) 986-6546, Email: sjh210@lehigh.edu

EDUCATION:

2010-Present:

M.Sc., Earth and Environmental Science
Lehigh University, Bethlehem Pennsylvania
GPA: 3.65
Thesis: "Postglacial Climate, Disturbance and Permafrost Peatland Dynamics on the Seward Peninsula, Western Alaska."
Masters Committee: Zicheng Yu, Bob Booth, Benjamin Felzer

2006-2010:

B.Sc., Earth and Environmental Science
Lehigh University, Bethlehem Pennsylvania
GPA 3.2; Major GPA: 3.5
Honors: Departmental Honors, Donnell Foster Hewitt Award
Thesis: "Response of Peatland Carbon Accumulation to Late Holocene Climate Change in South-Central Alaska."

PROFESSIONAL EXPERIENCE

Lehigh University
Teaching Assistant **August 2011-December 2011**

- Duties included organizing and managing lab classes, instructing students on proper procedures, moderating class discussions, and grading assignments

Lehigh University
Research Assistant **August 2010 – August 2011**

- Research assistant under Dr. Zicheng Yu managing databases, completing lab analyses, and evaluating data in addition to independent thesis research.

Lehigh University
Research/Field Assistant **May 2009 – August 2009**

- Research assistant under Dr. Zicheng Yu evaluating data, managing and building databases, conducting vegetation surveys, soil sampling, water sampling, and making field observations during a field season in Alaska.

Lehigh University
Graduate Symposium Committee **2010-Present**

- Responsibilities include organizing the annual graduate research symposium by collaborating with graduate students, professors, and various university personnel for the 60 people, all-day event.

PUBLICATIONS

Hunt, S. 2011. Response of Peatland Carbon Accumulation to Postglacial Climate Changes on the Seward Peninsula, Western Alaska. *Fall 2011 Meeting of the American Geophysical Union.* San Francisco, California, December, 2011 (contributed poster)

Hunt, S. 2011. Response of peatland carbon accumulation to Holocene warm climates on the Seward Peninsula, western Alaska. *41st International Arctic Workshop*, Montreal, Canada. Abstract Volume pages 153-155. March 2011. (contributed poster)

Yu, Z., Loisel, J., Brosseau, D., Beilman, D., Hunt, S. 2010. Global peatland dynamics since the Last Glacial Maximum. *Geophysical Research Letters;* 37: 5 PP

AWARDS

Lehigh University
Donnell Foster Hewitt Award **2010**
Presented to the student that displays the most professional promise in the field of Earth and Environmental Sciences.

Lehigh University
Runner-Up for Best Poster **2012**
Presented to the first runner-up for best poster for the poster session at the Graduate Student Research Symposium.

SKILLS

- Environmental sampling of soil, sediment, groundwater and surface water
- Familiar with wetland delineation, vegetation surveys, plant identification, and ecological assessments
- Experienced with peat core sampling and analyses, including macrofossil, pollen, and loss-on-ignition analysis
- Experience in soil and rock classification
- Knowledgeable on data evaluation, statistical analyses, and database management
- Capacity to produce technical deliverables
- Geologic/hydrogeologic cross sections and contour mapping
- Ability to work with ArcGIS, SigmaPlot, Tilia, Microsoft Office, and Adobe Illustrator